Mixing effects on 1S and 2S state heavy mesons in the light-front quark model

Ahmad Jafar Arifi[1,*] Ho-Meoyng Choi[2,†] Chueng-Ryong Ji[3,‡] and Yongseok Oh[4,1,§]

[1]*Asia Pacific Center for Theoretical Physics, Pohang, Gyeongbuk 37673, Korea*
[2]*Department of Physics Education, Teachers College, Kyungpook National University, Daegu 41566, Korea*
[3]*Department of Physics, North Carolina State University, Raleigh, North Carolina 27695-8202, USA*
[4]*Department of Physics, Kyungpook National University, Daegu 41566, Korea*

The mass spectra and wave functions of both 1S and 2S state heavy pseudoscalar (P) and vector (V) mesons are analyzed within the light-front quark model. Important empirical constraints employed in our analysis of the mass spectra and wave functions are the experimental mass-gap relation, $\Delta M_P > \Delta M_V$, where $\Delta M_{P(V)} = M_{P(V)}^{2S} - M_{P(V)}^{1S}$ and the hierarchy of the decay constants, $f_{1S} > f_{2S}$, between 1S and 2S meson states. We maintain the orthogonality of the trial wave functions of the 1S and 2S states in our variational calculation of the Hamiltonian with the Coulomb plus confining potentials and treat the hyperfine interaction perturbatively for the heavy-heavy and heavy-light P and V mesons due to the nature of the heavy quark symmetry. Realizing that the empirical constraints cannot be satisfied without mixing of the 1S and 2S states, we find the lower bound of the mixing angle θ between 1S and 2S states as $\theta_c = \cot^{-1}(2\sqrt{6})/2 \simeq 6°$ and obtain the optimum value of the mixing angle around 12° to cover both the charm and bottom flavors of the heavy quark. The mixing effects are found to be more significant to the 2S state mesons than to the 1S state mesons. The properties of 1S and 2S state mesons including the mass spectra, decay constants, twist-2 distribution amplitudes, and electromagnetic form factors are computed. Our results are found to be in a good agreement with the available data and lattice simulations. In particular, the 2S state pseudoscalar D_s meson is predicted to have a mass of 2600 MeV, which is very close to the mass of the newly discovered $D_{s0}(2590)^+$ meson by the LHCb Collaboration. This supports the interpretation of the observed state as a radial excitation of the D_s^+ meson.

I. INTRODUCTION

Quantum chromodynamics (QCD) is a unique theory of strong interactions with its nonperturbative nature in the low-energy regime and its asymptotically free nature in the high-energy regime. Building the effective degrees of freedom that describe the strongly interacting system in the low-energy regime is one of the crucial issues in understanding the link between the first-principle QCD and the constituent quark model (CQM) that has proven to provide successful and intuitive descriptions of hadrons.

*ahmad.jafar.arifi@apctp.org
†homyoung@knu.ac.kr
‡crji@ncsu.edu
§yohphy@knu.ac.kr

In particular, the light-front dynamics (LFD) is found to provide an effective way to handle the relativistic effects thanks to its distinguished features of the rational energy-momentum dispersion relation. It carries the maximum number (seven) of the kinetic (or interaction-independent) generators rendering the less effort in dynamics to get the QCD solutions that reflect the full Poincaré symmetries [1,2]. Effectively, the light-front quark model (LFQM) based on the LFD turns out to be one of the most successful hadronic models in describing various properties of hadrons.

While the LFQM analyses have been quite successful in describing the properties of ground state mesons [3–15], the structures and properties of the excited hadron states are yet to be understood in LFQM more extensively as their nature is still veiled and not well explored compared to the ground states. One of the most challenging problems in the quest of the excited states is to clarify whether the observed state belongs to the standard quark-antiquark excitation or an exotic state. For instance, the newly observed $D_{s0}(2590)^+$ meson with a mass of $2591 \pm 6 \pm 7$ MeV

by the LHCb Collaboration [16] has been proposed as a radial excitation of the D_s^+ meson. However, the observed mass is quite smaller than the available CQM predictions. For example, the relativized quark model of Ref. [17] predicts 2680 MeV and the relativistic quark model based on the quasipotential approach predicts 2688 MeV [18,19]. In recent works, therefore, some modifications by including screening effects in the potential [20] and some nonstandard quark-antiquark behaviors [21,22] attributed to this resonance have been discussed to explain the data.

In particular, the radially excited states of hadrons are important in understanding the strong interactions as they give information complementary to the orbitally excited states. They have been observed in light and heavy quark sectors of hadrons although some of them are yet to be confirmed according to the Particle Data Group (PDG) [23]. The most well-known example in baryon spectrum is the Roper resonance [24]. Such states with multistrangeness were recently discussed in Ref. [25], and the excited states in meson spectrum were discussed and summarized, for example, in Ref. [26]. Most notable empirical hierarchy appears in the radially excited $2S$ state as well as the ground $1S$ state of heavy pseudoscalar (P) and vector (V) mesons. Namely, the two important constraints that we notice from the empirical hierarchy are (i) the experimental mass gap relation $\Delta M_P > \Delta M_V$, where $\Delta M_{P(V)} = M_{P(V)}^{2S} - M_{P(V)}^{1S}$, and (ii) the hierarchy of the decay constants $f_{1S} > f_{2S}$. While these constraints on the mass spectra and the decay constants apply both for the light and heavy meson sectors, the difference between P and V becomes much larger in the light meson sectors. The reason for the smaller difference between P and V in the heavy-light system may well be attributed to the heavy quark symmetry [27–30]. Moreover, the hyperfine interaction can be handled perturbatively in the heavy quark systems because the hyperfine interaction is suppressed by the masses of heavy quarks. This may be contrasted with the chiral symmetry reflected in the light meson sectors, which deserves a separate analysis and discussion. Due to these significant differences in the underlying symmetry between the light and heavy meson sectors, we apply the two constraints here only for the heavy meson sectors and discuss the heavy-heavy and heavy-light P and V mesons in the present work. Effectively, we analyze the mass spectra and wave functions of the radially excited $2S$ state and the ground $1S$ state of heavy P and V meson sectors within the framework of the LFQM and discuss various properties of these mesons.

In the previous LFQM analyses of the mass spectra and decay constants of the $1S$ state mesons performed by two of us with the QCD-motivated effective Hamiltonian [10–15], the trial wave functions were chosen as either the pure harmonic oscillator (HO) wave function ϕ_{1S} [10–13] or an expansion in the HO basis functions, i.e., $\Phi = \sum_{n=1}^{n_{\max}} c_n \phi_{nS}$ with $n_{\max} = 2$ [14] or 3 [15]. Through the analyses of the $1S$ state mesons, it was shown that the physical observables

are not much sensitive to the number of HO bases used in the trial wave functions, $\Phi = \sum_{n=1}^{n_{\max}} c_n \phi_{nS}$, once the optimum values of the model parameters are fitted. For the combined analysis of $(1S, 2S)$ state heavy mesons in the present work, we take into account the two important constraints in obtaining the optimum values of our model parameters. We note that f_{nS} tends to be smaller as n gets larger since the decay constant of a hadron is proportional to its radial wave function at the origin, $\psi(r = 0)$. The available experimental data have also confirmed this tendency. In the literature, however, some difficulties in the combined analysis of the ground and radially excited states have been observed. For instance, in the LFQM analysis of $(1S, 2S)$ state heavy $\Upsilon(b\bar{b})$ systems, it was found that using the HO wave functions ϕ_{nS} ($n = 1, 2$) leads to the reverse order problem of $f_{1S} < f_{2S}$ [7]. In order to resolve this problem and to obtain the correct hierarchy of $f_{1S} > f_{2S}$ for the heavy quarkonium system using two pure (ϕ_{1S}, ϕ_{2S}) wave functions, the authors of Refs. [31,32] had to choose different HO model parameters for different nS states, which breaks the orthogonality condition between the two wave functions ϕ_{1S} and ϕ_{2S}. A similar problem, namely, the breakdown of orthogonality condition between the resultant $1S$ and $2S$ state light-front (LF) wave functions, appears in the analysis of heavy quarkonium system performed with the basis light-front quantization (BLFQ) approach in a holographic basis [33].

The main purpose of the present work is thus to extend the previous LFQM analyses including both $1S$ and $2S$ state P and V heavy meson sectors to remedy the difficulties in the combined analysis using the trial wave functions for $1S$ and $2S$ states as mixtures of the two HO wave functions ϕ_{1S} and ϕ_{2S}. In particular, our trial wave functions for $1S$ and $2S$ states satisfy naturally the orthogonality condition. One of the key findings in this work is the criterion of the mixing angle between ϕ_{1S} and ϕ_{2S} for reproducing the correct order of the mass gap (i.e., $\Delta M_P > \Delta M_V$) and decay constants (i.e., $f_{1S} > f_{2S}$) between $1S$ and $2S$ states. Various properties of heavy $(1S, 2S)$ state mesons such as mass spectra, decay constants, distribution amplitudes (DAs), and electromagnetic form factors are also scrutinized. Moreover, we obtain the mass of the radially excited $D_s(2S)$ state as $M \approx 2600$ MeV, which leaves the possibility that the $D_{s0}(2590)^+$ observed recently by the LHCb Collaboration [16] can be interpreted as the standard quark-antiquark radial excitation.

This paper is organized as follows. In Sec. II, we briefly introduce the effective Hamiltonian and the trial wave functions adopted in the present approach. We then describe how to determine the model parameters via the variational analysis. Subsequently, we describe the mass spectra of the $1S$ and $2S$ state heavy mesons discussing the role of the mixing. In Sec. III, we summarize various properties of heavy mesons including decay constants, DAs, and electromagnetic form factors obtained in our

LFQM formalism. Section IV presents our numerical results for those quantities of $(1S, 2S)$ state heavy pseudoscalar and vector mesons. Finally, we summarize and conclude in Sec. V.

II. MODEL DESCRIPTION

The key idea in our LFQM [10–14] for the $1S$ state mesons is to treat the radial wave function as a trial function for the variational principle to the QCD-motivated effective Hamiltonian saturating the Fock state expansion by the constituent quark and antiquark. In this section, we briefly summarize our LFQM and discuss some distinguished features for the trial wave functions and their mixing angles that emerge from the inclusion of the radially excited $2S$ state in addition to the $1S$ state.

A. Effective Hamiltonian

The meson system at rest is described as an interacting bound system of effectively dressed valence quark and antiquark satisfying the eigenvalue equation of the QCD-motivated effective Hamiltonian,

$$H_{q\bar{q}}|\Psi_{q\bar{q}}\rangle = M_{q\bar{q}}|\Psi_{q\bar{q}}\rangle, \tag{1}$$

where $M_{q\bar{q}}$ and $\Psi_{q\bar{q}}$ are the mass eigenvalue and eigenfunction of the $q\bar{q}$ meson state, respectively. We take the Hamiltonian $H_{q\bar{q}}$ in the quark-antiquark center of mass frame as

$$H_{q\bar{q}} = H_0 + V_{q\bar{q}} = \sqrt{m_q^2 + \mathbf{k}^2} + \sqrt{m_{\bar{q}}^2 + \mathbf{k}^2} + V_{q\bar{q}}, \tag{2}$$

where H_0 is the kinetic energy part of the quark and antiquark with three-momentum $\mathbf{k} = (\mathbf{k}_\perp, k_z)$. The effective potential $V_{q\bar{q}}$ is given by [10–13]

$$V_{q\bar{q}} = V_{\text{Conf}} + V_{\text{Coul}} + V_{\text{Hyp}}, \tag{3}$$

where V_{Conf} is the linear confining potential,

$$V_{\text{Conf}} = a + br \tag{4}$$

with a and b being parameters to be determined later. The Coulomb potential and hyperfine interaction potential stemming from the effective one-gluon exchanges for the S-wave mesons are respectively

$$V_{\text{Coul}} = -\frac{4\alpha_s}{3r}, \qquad V_{\text{Hyp}} = \frac{2}{3}\frac{\mathbf{S}_q \cdot \mathbf{S}_{\bar{q}}}{m_q m_{\bar{q}}}\boldsymbol{\nabla}^2 V_{\text{Coul}}. \tag{5}$$

Here, $\langle \mathbf{S}_q \cdot \mathbf{S}_{\bar{q}} \rangle$ is $1/4$ and $-3/4$ for vector and pseudoscalar mesons, respectively, and we take the strong coupling α_s as a variation parameter. As we consider the heavy meson sector in this work, we handle V_{Hyp} perturbatively employing the contact hyperfine interaction, i.e.,

$\boldsymbol{\nabla}^2 V_{\text{Coul}} = (16\pi\alpha_s/3)\delta^3(\mathbf{r})$, which is a fairly good approximation for the analysis of heavy meson mass spectroscopy.

The LF wave function is represented by the Lorentz invariant internal variables $x_i = p_i^+/P^+$, $\mathbf{k}_{\perp i} = \mathbf{p}_{\perp i} - x_i \mathbf{P}_\perp$, and helicity λ_i, where $P^\mu = (P^+, P^-, \mathbf{P}_\perp)$ is the four-momentum of the meson and p_i^μ is the four-momentum of the ith $(i = 1, 2)$ constituent quark, which leads to the constraints $\sum_{i=1}^2 x_i = 1$ and $\sum_{i=1}^2 \mathbf{k}_{\perp i} = 0$. We assign $i = 1$ to the quark and $i = 2$ to the antiquark, and define $x \equiv x_1$ and $\mathbf{k}_\perp \equiv \mathbf{k}_{\perp 1}$. Then, the three-momentum $\mathbf{k} = (k_z, \mathbf{k}_\perp)$ can be written as $\mathbf{k} = (x, \mathbf{k}_\perp)$ via the relation,

$$k_z = \left(x - \frac{1}{2}\right)M_0 + \frac{m_{\bar{q}}^2 - m_q^2}{2M_0}, \tag{6}$$

where

$$M_0^2 = \frac{\mathbf{k}_\perp^2 + m_q^2}{x} + \frac{\mathbf{k}_\perp^2 + m_{\bar{q}}^2}{1 - x} \tag{7}$$

is the boost-invariant meson mass squared. Therefore, the variable transformation $\{k_z, \mathbf{k}_\perp\} \to \{x, \mathbf{k}_\perp\}$ accompanies the Jacobian factor,

$$\frac{\partial k_z}{\partial x} = \frac{M_0}{4x(1-x)}\left[1 - \frac{(m_q^2 - m_{\bar{q}}^2)^2}{M_0^4}\right], \tag{8}$$

which we take into account for the normalization of the radial part of the wave function.

The LF wave function $\Psi_{q\bar{q}} = \Psi_{nS}^{JJ_z}$ of the nS state pseudoscalar and vector mesons in the momentum space is then given by

$$\Psi_{nS}^{JJ_z}(x, \mathbf{k}_\perp, \lambda_i) = \Phi_{nS}(x, \mathbf{k}_\perp)\mathcal{R}_{\lambda_q \lambda_{\bar{q}}}^{JJ_z}(x, \mathbf{k}_\perp), \tag{9}$$

where $\Phi_{nS}(x, \mathbf{k}_\perp)$ is the radial wave function and $\mathcal{R}_{\lambda_q \lambda_{\bar{q}}}^{JJ_z}$ is the spin-orbit wave function that is obtained by the interaction-independent Melosh transformation from the ordinary spin-orbit wave function assigned by the quantum number J^{PC}. The covariant forms of $\mathcal{R}_{\lambda_q \lambda_{\bar{q}}}^{JJ_z}$ for pseudoscalar and vector mesons are given by [3]

$$\mathcal{R}_{\lambda_q \lambda_{\bar{q}}}^{00} = -\frac{1}{\sqrt{2}\tilde{M}_0}\bar{u}_{\lambda_q}(p_q)\gamma_5 v_{\lambda_{\bar{q}}}(p_{\bar{q}}),$$

$$\mathcal{R}_{\lambda_q \lambda_{\bar{q}}}^{1J_z} = -\frac{1}{\sqrt{2}\tilde{M}_0}\bar{u}_{\lambda_q}(p_q)\left[\not{\epsilon}(J_z) - \frac{\epsilon \cdot (p_q - p_{\bar{q}})}{M_0 + m_q + m_{\bar{q}}}\right]v_{\lambda_{\bar{q}}}(p_{\bar{q}}), \tag{10}$$

where $\tilde{M}_0 \equiv \sqrt{M_0^2 - (m_q - m_{\bar{q}})^2}$. The polarization vectors $\epsilon^\mu(J_z) = (\epsilon^+, \epsilon^-, \boldsymbol{\epsilon}_\perp)$ of the vector meson are given by [3]

$$\epsilon^\mu(\pm 1) = \left(0, \frac{2}{P^+}\boldsymbol{\epsilon}_\perp(\pm)\cdot\mathbf{P}_\perp, \boldsymbol{\epsilon}_\perp(\pm)\right),$$

$$\epsilon^\mu(0) = \frac{1}{M_0}\left(P^+, \frac{-M_0^2 + \mathbf{P}_\perp^2}{P^+}, \mathbf{P}_\perp\right), \qquad (11)$$

where

$$\boldsymbol{\epsilon}_\perp(\pm 1) = \mp\frac{1}{\sqrt{2}}(1, \pm i), \qquad (12)$$

so that the spin-orbit wave functions $\mathcal{R}_{\lambda_q\lambda_{\bar{q}}}^{JJ_z}$ satisfy the unitary condition automatically, i.e., $\langle\mathcal{R}_{\lambda_q\lambda_{\bar{q}}}^{JJ_z}|\mathcal{R}_{\lambda_q\lambda_{\bar{q}}}^{JJ_z}\rangle = 1$.

For the $1S$ and $2S$ state radial wave functions Φ_{ns} of Eq. (9), we allow the mixing between the two lowest order HO wave functions (ϕ_{1S}, ϕ_{2S}) by writing

$$\begin{pmatrix}\Phi_{1S}\\\Phi_{2S}\end{pmatrix} = \begin{pmatrix}\cos\theta & \sin\theta\\-\sin\theta & \cos\theta\end{pmatrix}\begin{pmatrix}\phi_{1S}\\\phi_{2S}\end{pmatrix}, \qquad (13)$$

where

$$\phi_{1S}(x, \mathbf{k}_\perp) = \frac{4\pi^{3/4}}{\beta^{3/2}}\sqrt{\frac{\partial k_z}{\partial x}}e^{-\mathbf{k}^2/2\beta^2},$$

$$\phi_{2S}(x, \mathbf{k}_\perp) = \frac{4\pi^{3/4}}{\sqrt{6}\beta^{7/2}}(2\mathbf{k}^2 - 3\beta^2)\sqrt{\frac{\partial k_z}{\partial x}}e^{-\mathbf{k}^2/2\beta^2}, \quad (14)$$

and β is the parameter which is inversely proportional to the range of the wave function and can be used as the variational parameter in our mass spectroscopic analysis. It should be noted that the wave functions ϕ_{nS} include the Jacobian factor $\partial k_z/\partial x$ so that the HO bases ϕ_{nS} satisfy the following normalization:

$$\int_0^1 dx \int \frac{d^2\mathbf{k}_\perp}{2(2\pi)^3}|\phi_{nS}(x, \mathbf{k}_\perp)|^2 = 1. \qquad (15)$$

From the orthonormality of $\Phi_{nS}(n = 1, 2)$ defined in Eq. (13) and the unitarity of $\mathcal{R}_{\lambda_q\lambda_{\bar{q}}}^{JJ_z}$, one can easily see that Φ_{nS} and $\Psi_{nS}^{JJ_z}$ of Eq. (9) satisfy the same normalization as ϕ_{nS}. We denote (Φ_{1S}, Φ_{2S}) for $\theta \neq 0$ and $(\Phi_{1S}, \Phi_{2S}) = (\phi_{1S}, \phi_{2S})$ for $\theta = 0$ as "mixed" and "pure" $(1S, 2S)$ states, respectively. As we shall discuss below, the mixing scheme turns out to be crucial to reproduce the experimental data for both masses and decay constants of heavy mesons.

B. Variational method to effective Hamiltonian

The present LFQM for the combined analysis of the $1S$ and $2S$ state heavy mesons has several parameters, namely, the constituent quark masses (m_q, m_s, m_c, m_b) with m_q being the light u or d quark mass, the potential parameters (a, b, α_s), the HO parameter β for each $(q\bar{q})$ content, and the mixing angle θ. We first determine the values of these parameters by reproducing the mass spectra based on the variational principle. Then, we compute other observables of heavy mesons such as decay constants, DAs, and electromagnetic form factors.

Here we follow the procedure adopted in Refs. [10–13], namely, we consider the central potential $V_0 = V_{\text{Conf}} + V_{\text{Coul}}$ as well as the kinetic energy H_0 in the variational calculation via

$$\frac{\partial\langle\Psi_{q\bar{q}}|(H_0 + V_0)|\Psi_{q\bar{q}}\rangle}{\partial\beta} = 0. \qquad (16)$$

Then, the remaining $\langle\Psi_{q\bar{q}}|V_{\text{hyp}}|\Psi_{q\bar{q}}\rangle$ is treated as a perturbation so that we have β values common for both pseudoscalar and vector mesons of the same $(q\bar{q})$ content. This constrains the model parameters. Since the spin-orbit wave function satisfies the exact unitarity, we have the mass eigenvalue of the meson as $M_{q\bar{q}} = \langle\Psi_{q\bar{q}}|H_{q\bar{q}}|\Psi_{q\bar{q}}\rangle = \langle\Phi_{nS}|H_{q\bar{q}}|\Phi_{nS}\rangle$. The analytic forms of the mass eigenvalues $(M_{q\bar{q}}^{1S}, M_{q\bar{q}}^{2S})$ for the mixed $(1S, 2S)$ state mesons are then obtained as

$$M_{q\bar{q}}^{1S} = \frac{\beta}{\sqrt{\pi}}\sum_{i=q,\bar{q}}\left\{z_i e^{z_i/2}\left[\frac{1}{3}c_2^2(3 - z_i)z_i K_2\left(\frac{z_i}{2}\right) + \frac{1}{6}(9 - 3c_1^2 + 2c_2^2 z_i^2 - 6\sqrt{6}c_1 c_2)K_1\left(\frac{z_i}{2}\right)\right]\right.$$

$$\left. + \sqrt{\pi}(\sqrt{6}c_1 c_2 - 3c_2^2)U(-1/2, -2, z_i)\right\}$$

$$+ a + \frac{b}{\beta\sqrt{\pi}}\left(3 - c_1^2 - 2\sqrt{\frac{2}{3}}c_1 c_2\right) - \frac{4\alpha_s\beta}{9\sqrt{\pi}}\left(5 + c_1^2 + 6\sqrt{\frac{2}{3}}c_1 c_2\right) + \frac{16\alpha_s\beta^3\langle\mathbf{S}_q\cdot\mathbf{S}_{\bar{q}}\rangle}{9m_q m_{\bar{q}}\sqrt{\pi}}(3 - c_1^2 + 2\sqrt{6}c_1 c_2),$$

$$M_{q\bar{q}}^{2S} = M_{q\bar{q}}^{1S}(c_1 \to -c_2, c_2 \to c_1), \qquad (17)$$

where $(c_1, c_2) = (\cos\theta, \sin\theta)$, $z_i = m_i^2/\beta^2$, $K_n(x)$ is the modified Bessel function of the second kind of order n, and $U(a, b, z)$ is the Tricomi's (confluent hypergeometric) function. The mass eigenvalues for the pure $(1S, 2S)$ states can be read by setting $\theta = 0$, i.e., $(c_1 = 1, c_2 = 0)$ in Eq. (17).

In order to explore the mixing effects and to determine the optimal value of the mixing angle θ, we utilize the empirical constraint on the mass gap $\Delta M_{P(V)} = M_{P(V)}^{2S} - M_{P(V)}^{1S}$ between the $1S$ and $2S$ state heavy pseudoscalar and

vector mesons. The mass gap $\Delta M_{P(V)}$ for pseudoscalar (vector) mesons in our LFQM is decomposed as

$$\Delta M_{P(V)} = \Delta M_{P(V)}^{\text{Kin}} + \Delta M_{P(V)}^{\text{Conf}} + \Delta M_{P(V)}^{\text{Coul}} + \Delta M_{P(V)}^{\text{Hyp}}, \quad (18)$$

where we separate the four different contributions, i.e., H_0, V_{Conf}, V_{Coul}, and V_{Hyp}, to the total mass gap for the taxonomical analysis in our numerical calculations. From the available experimental data for the $1S$ and $2S$ state heavy meson pairs, (D, D^*), $(\eta_c, J/\Psi)$, and (η_b, Υ) [23], we observe that the mass gaps between pseudoscalar mesons (ΔM_P) are greater than the corresponding mass gaps between vector mesons (ΔM_V), i.e., $\Delta M_P > \Delta M_V$. In our LFQM calculation, $\Delta M_P^{\text{Kin+Conf+Coul}} = \Delta M_V^{\text{Kin+Conf+Coul}}$ due to the usage of common β parameters for both pseudoscalar and vector mesons of the same quark flavor contents as shown in Eq. (17), and thus the mass gap is exclusively governed by the hyperfine interaction V_{Hyp} and can be readily obtained as

$$
\begin{aligned}
\Delta M_P - \Delta M_V &= \Delta M_P^{\text{Hyp}} - \Delta M_V^{\text{Hyp}} \\
&= C(2\sqrt{6}\sin 2\theta - \cos 2\theta), \quad (19)
\end{aligned}
$$

where $C = 16\alpha_s\beta^3/(9m_q m_{\bar{q}}\sqrt{\pi})$.

Equation (19) combined with the relation $\Delta M_P > \Delta M_V$ provides a very important constraint on the mixing angle θ. It is evident that the pure (ϕ_{1S}, ϕ_{2S}) states with $\theta = 0°$ always leads to $\Delta M_P < \Delta M_V$, which shows that the introduction of the mixing is inevitable. Furthermore, one can find that the condition of $\Delta M_P > \Delta M_V$ gives the constraint,

$$\frac{1}{2}\cot^{-1}(2\sqrt{6}) < \theta < \frac{\pi}{4}. \quad (20)$$

This concludes that the lower bound of the physical mixing angle, θ_c, is determined as $\theta > \theta_c = \cot^{-1}(2\sqrt{6})/2 \simeq 6°$.

C. Model parameters

As we have discussed in the previous subsection, the parameters of heavy mesons in the present model for $(1S, 2S)$ state mesons include four quark masses (m_q, m_s, m_c, m_b) with $(q = u, d)$, seven variational HO parameters $(\beta_{qc}, \beta_{sc}, \beta_{qb}, \beta_{sb}, \beta_{cc}, \beta_{cb}, \beta_{bb})$, three potential parameters (a, b, α_s), and the mixing angle θ. The variational principle in Eq. (16) leads to a constraint in the parameter space,

which relates the strong coupling constant α_s and the other parameters, i.e., $\alpha_s = \alpha_s(\theta, a, b, m_q, m_{\bar{q}}, \beta_{q\bar{q}})$. This indicates that the variational parameters $\beta_{q\bar{q}}$ are automatically determined once other model parameters such as the quark masses, the strong coupling constant, the string tension, and the mixing angle are fixed.

In this study of heavy mesons, we take $m_q = 0.22$ GeV, $m_s = 0.45$ GeV, and the widely-used string tension $b = 0.18$ GeV^2 [17,34,35] as inputs, which were adopted in our previous LFQM analysis [10–13] for the $1S$ state mesons. This leaves five parameters, i.e., $(m_c, m_b, a, \alpha_s, \theta)$, to be determined. In order to determine those five unknowns, we use two masses of the $1S$ state heavy mesons as inputs. Among many possible choices of two input masses, we find that the use of the (η_b, B^*) pair masses as inputs produces other meson masses well enough compared to the data. Since we have only two equations (M_{η_b}, M_{B^*}) with five unknowns to be determined, we first try to find the best fit parameters for the pure $(1S, 2S)$ state case without mixing $(\theta = 0°)$. In this case, we need to choose two input parameters from (m_c, m_b, a, α_s). Through our analyses with various combinations, we found that $m_c = 1.68$ GeV and $m_b = 5.10$ GeV give satisfactory results. We then obtain the remaining potential parameters, $a = -0.538$ GeV and $\alpha_s = 0.425$, by solving Eq. (17) for $(M_{\eta_b}^{1S}, M_{B^*}^{1S})$ using their measured values. We also note that V_{Conf} and V_{Coul} are flavor- and scale-independent so that the confining potential constant a and the strong coupling α_s are the same for all heavy mesons considered in this work. Therefore, once a and α_s are determined, the values of seven β parameters are automatically computed and all the other meson masses are our predictions.

Using the same quark masses (m_q, m_s, m_c, m_b) and the string tension b as in the $\theta = 0°$ case but taking into account of the two experimental constraints, $\Delta M_P^{\text{Hyp}} > \Delta M_V^{\text{Hyp}}$ and $f_{1S} > f_{2S}$, we obtain the optimum value $\theta = 12°$ of the mixing angle as well as other model parameters to cover both charm and bottom flavors of the heavy quark. We should note that the mixing angle in general depends on the quark flavor contents of mesons, e.g., we find $\theta = 9.8°$, $17.6°$, and $13.9°$ for (D, D^*), $(\eta_c, J/\Psi)$, and (η_b, Υ), using the measured masses [23] and the potential model parameters in Table I, respectively. The paucity of data however does not allow us to estimate the mixing angles for the other mesons. The scope of this work is thus not to use all the different mixing angles in our heavy meson analysis but to explain the observed experimental data for various physical

TABLE I. The constituent quark masses, potential parameters (a, b, α_s), and variational parameters $\beta_{q\bar{q}}$ for the pure and mixed scenarios. The quark masses, potential parameter a, and variational parameters β are in the units of GeV, while the string constant b is in the unit of GeV^2. The strong coupling α_s is dimensionless and $q = u, d$.

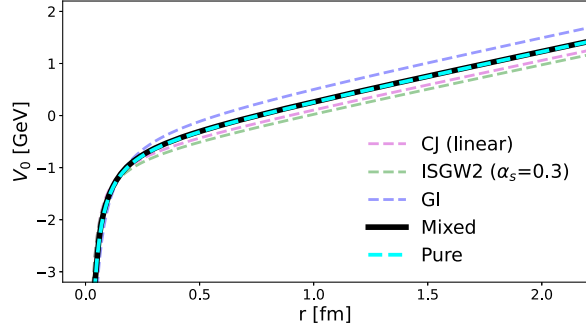| Mixing angle	m_q	m_s	m_c	m_b	b	a	α_s	β_{qc}	β_{sc}	β_{qb}	β_{sb}	β_{cc}	β_{cb}	β_{bb}
Pure $(\theta = 0°)$	0.22	0.45	1.68	5.10	0.18	−0.538	0.425	0.500	0.537	0.585	0.636	0.699	0.906	1.376
Mixed $(\theta = 12°)$						−0.543	0.433	0.424	0.455	0.495	0.538	0.592	0.767	1.167

FIG. 1. Central potentials in two different scenarios, the pure and mixed configurations. No noticeable difference is observed between these two cases. The potentials of the CJ [13], ISGW2 [35], and GI [17] models are presented for comparison.

observables such as mass spectra, decay constants, and the electromagnetic form factors etc., with the minimal model parameters without losing the predictive power of our model computation. In this respect, we try to find the optimum value of the mixing angle by analyzing not only the mass spectra satisfying the experimental mass gap relation ($\Delta M_P > \Delta M_V$) but also decay constants satisfying $f_{1S} > f_{2S}$. We also contrast between the pure vs mixed cases to exhibit possible uncertainties associated with the use of the optimum mixing angle. This would be enough for verifying the mixing effects on the physical quantities of heavy mesons.

We summarize our best fits for the model parameters obtained for the mixed state ($\theta = 12°$) case in Table I. For

the comparison purpose of mixing effects, we also include the best fits for the model parameters obtained for the pure state ($\theta = 0°$) case. This shows that the values of a and α_s are not significantly different in both cases, but the values of the β parameters become smaller with mixing, which results in different meson properties.

With the model parameters determined above, we can compare the central potential V_0 with other model calculations. In Fig. 1, we present the central potentials $V_0(r)$ up to $r \simeq 2$ fm for the pure and mixed configurations ($\theta = 0°$ and $12°$, respectively) and compare them with the well-known GI model [17] and ISGW2 model [35]. We also plot the potential of the previous works by two of us in Refs. [10–13] as the CJ model. As one may expect from the similarities of the model parameters (a, b, α_s), the central potentials obtained from the two different mixing scenarios are almost the same and they are also quite comparable with the results from the GI and ISGW2 models as well as the CJ model.

The mixing effects on the $1S$ and $2S$ state radial wave functions are shown in Fig. 2 for the bottomonium ($b\bar{b}$) case. In Figs. 2(a) and 2(b), we compare the two radial wave functions of the pure ϕ_{nS} states (dashed lines) and the mixed Φ_{nS} states (solid lines) for $n = 1, 2$. Shown in Fig. 2(c) are the ratios $R_\phi = \phi_{2S}^2/\phi_{1S}^2$ (dashed line) and $R_\Phi = \Phi_{2S}^2/\Phi_{1S}^2$ (solid line). This shows that the small mixing ($\theta = 12°$) significantly modifies the wave function of the $2S$ state, while the $1S$ radial wave function is barely modified. The mixed state radial wave functions Φ_{nS} and their ratios for
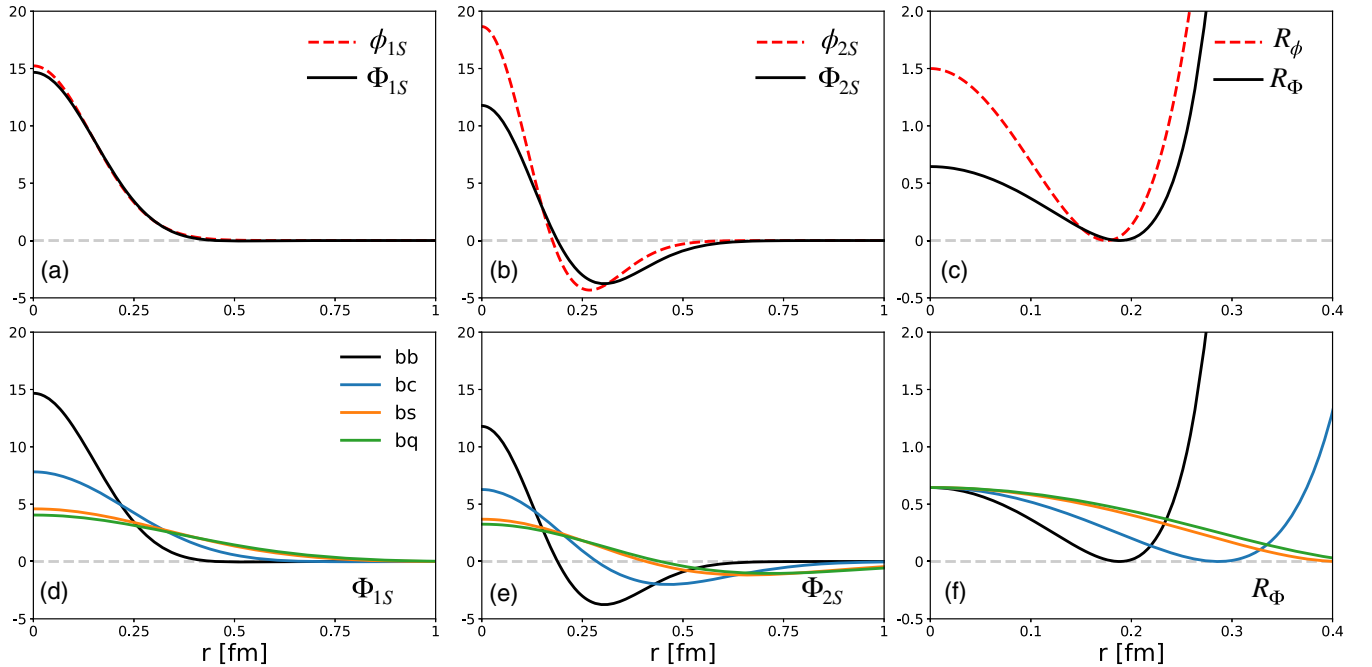

FIG. 2. Upper: radial wave functions in the pure and mixed configurations for the bottomonium $b\bar{b}$ states. The mixing modifies the $2S$ wave function significantly, while the $1S$ wave function is barely unchanged. The ratio is defined by $R_\phi = \phi_{2S}^2/\phi_{1S}^2$ and $R_\Phi = \Phi_{2S}^2/\Phi_{1S}^2$. Lower: radial wave functions in mixed scenario for various quark flavor contents.

TABLE II.   Mass spectra of the 1S and 2S state heavy mesons in the units of MeV.

State	Pure ($\theta = 0°$)	Mixed ($\theta = 12°$)	Expt. [23]	GI [17]	RQM [18,19]
$D(1S)$	1731	1745	1869.66(05)	1880	1871
$D(2S)$	2282	2432	2549(19)	2580	2581
$D^*(1S)$	2020	2017	2010.26(05)	2040	2010
$D^*(2S)$	2714	2608	2627(10)	2640	2632
$D_s(1S)$	1938	1946	1968.35(7)	1980	1969
$D_s(2S)$	2546	2600	2591(6)[a]	2670	2688
$D_s^*(1S)$	2113	2111	2112.2(4)	2130	2111
$D_s^*(2S)$	2798	2706	2714(5)	2730	2731
$\eta_c(1S)$	2987	2990	2983.9(4)	2970	2979
$\eta_c(2S)$	3627	3608	3637.5(1.1)	3620	3588
$J/\Psi(1S)$	3090	3087	3096.900(6)	3100	3096
$\Psi(2S)$	3781	3670	3686.10(6)	3680	3686
$B(1S)$	5174	5182	5279.34(12)	5310	5280
$B(2S)$	5740	5794	…	5900	5890
$B^*(1S)$	5325	5325	5324.70(21)	5370	5326
$B^*(2S)$	5968	5886	…	5930	5906
$B_s(1S)$	5325	5330	5366.88(14)	5390	5372
$B_s(2S)$	5924	5928	…	5980	5976
$B_s^*(1S)$	5421	5418	$5415.4^{+1.8}_{-1.5}$	5450	5414
$B_s^*(2S)$	6067	5987	…	6010	5992
$B_c(1S)$	6269	6270	6274.47(32)	6270	6270
$B_c(2S)$	6948	6885	…	6850	6835
$B_c^*(1S)$	6270	6340	…	6340	6332
$B_c^*(2S)$	7059	6930	…	6890	6881
$\eta_b(1S)$	9399	9399	9398.7(2.0)	9400	9400
$\eta_b(2S)$	10249	10123	9999(4)	9980	9993
$\Upsilon(1S)$	9485	9480	9460.30(26)	9460	9460
$\Upsilon(2S)$	10377	10175	10023.26(31)	10000	10023

[a]From the recent observation by the LHCb Collaboration [16].

various heavy-heavy ($b\bar{b}$, $b\bar{c}$) and heavy-light ($b\bar{s}$, $b\bar{q}$) with ($q = u$, d) quark states are also given in Figs. 2(d)–2(f). Since the range of the radial wave function is inversely proportional to the value of the β parameter, it is quite natural to observe that the wave function of bottomonium state is narrower than the other states. We also note that the value of the radial wave function at the origin ($r = 0$) is proportional to the β parameter. As shown in Figs. 2(d) and 2(e), the bottomonium wave function at the origin is the highest among those of meson wave functions for both the 1S and 2S states. However, the ratio R_Φ at the origin takes the same value independent of the quark flavor contents once the mixing angle is fixed as can be seen in Fig. 2(f).

D. Mass spectra

In this subsection, we compute the mass spectra of the 1S and 2S state heavy mesons. With the parameters given in Table I, the mass formulas in Eq. (17) are used to obtain the mass spectra. The meson masses obtained for $\theta = 0°$ and $\theta = 12°$ cases are summarized in Table II. As discussed before, all the meson masses apart from the two inputs

$(M_{\eta_b}^{1S}, M_{B^*}^{1S})$ are our predictions. For comparison, we also list the experimental data of Ref. [23] and the predictions of the GI model [17] and those of the relativistic quark model (RQM) in Refs. [18,19]. Our predictions obtained from both mixing scenarios are found to be overall in a good agreement with the experimental data [23]. However, there are some delicate but important mixing effects in mass spectra. While there are no big differences in the predicted masses for the 1S state mesons between the pure and mixed scenarios, the predictions for the 2S state mesons obtained from the mixed case agree better with the experimental data. This also can be seen by performing χ^2 analysis, which gives $\chi^2 = 0.009$ for the mixed scenario and $\chi^2 = 0.024$ for the pure one.[1]

In particular, our result, $M_{D_s(2S)} = 2600$ MeV for the 2S state of the D_s meson with $\theta = 12°$ is very close to the observed mass of the recently discovered $D_{s0}(2590)^+$ with

---

[1]The χ^2 is computed as $\chi^2 = \sum_i [(O_i - E_i)^2 / E_i^2]$, where O_i and E_i are the experimental data and theoretical prediction, respectively.
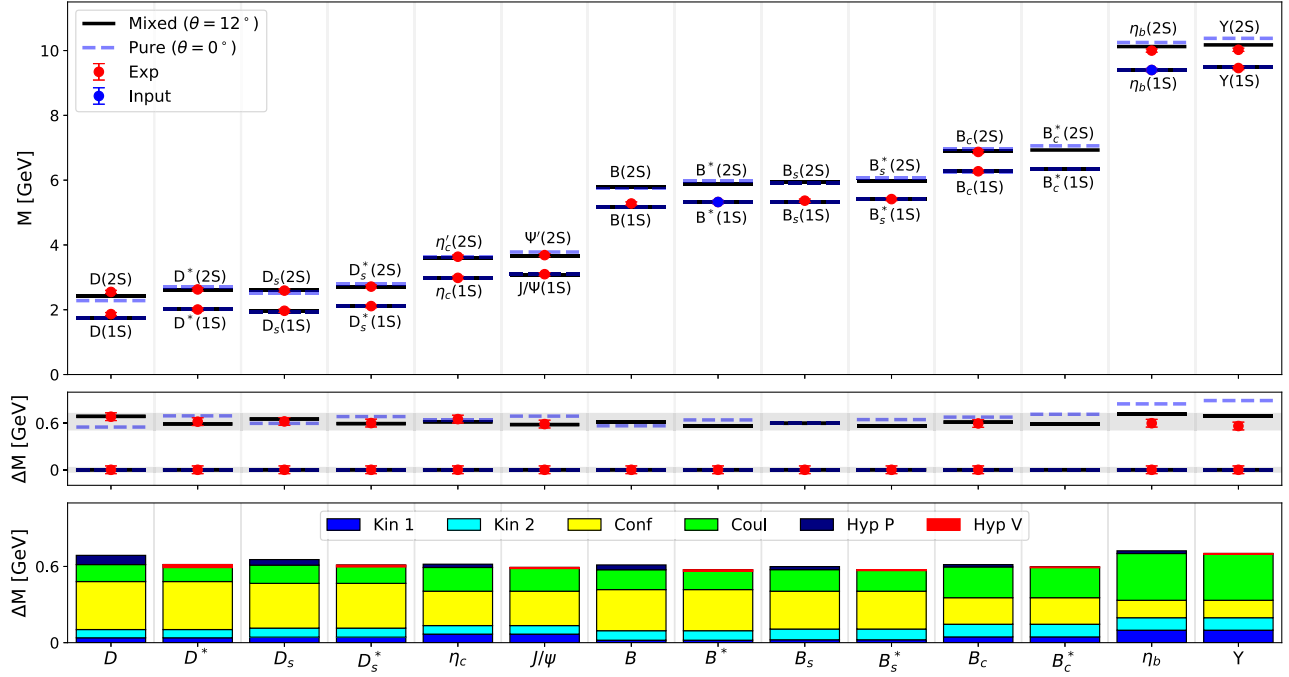
FIG. 3.   Upper: mass spectra of 1S and 2S state heavy mesons in the pure and mixed configurations. The experimental data are taken from Ref. [23] and the recent observation of the LHCb Collaboration [16]. Middle: the mass gap between the 1S and 2S heavy mesons. The masses of all the 2S states are given relative to the 1S state masses. The mass gap is observed to be around 600 MeV regardless of the quark flavor contents. Lower: the computed component of the mass gap. When the quark and antiquark have different masses, the contribution of the heavier (lighter) quark in H_0 is denoted as Kin 1 (Kin 2). Due to the negative sign of Hyp V contribution, the portion in red should be understood as a subtracted part not as an added part.

$J^P = 0^-$ [16]. This supports the interpretation of the observed $D_{s0}(2590)^+$ state as a standard quark-antiquark radial excitation of the D_s^+ meson as claimed by the LHCb Collaboration [16]. For making a definite conclusion on the structure of the $D_{s0}(2590)^+$, however, we still need more detailed and precise experimental studies on various properties of the $D_{s0}(2590)^+$.

The LHCb Collaboration [36] also reported traces of $B_J(5840)$ and $B_J(5960)$, and confirmed the observation of the $B_J(5960)$ by the CDF Collaboration [37]. Although their existence as resonances awaits confirmation and their quantum numbers are yet to be identified, these states are suggested as the 2S states of B and B^* mesons in Ref. [36]. However, if these are the $B(2S)$ and $B^*(2S)$ states, then it violates the mass hierarchy by giving $\Delta M_P < \Delta M_V$ as $\Delta M_P \approx 561$ MeV and $\Delta M_V \approx 635$ MeV. This is in contradiction with our predictions on the mass gaps, $\Delta M_P \approx 612$ MeV and $\Delta M_V \approx 561$ MeV, which observe the relation $\Delta M_P > \Delta M_V$. Therefore, verifying the $B(2S)$ and $B^*(2S)$ states is crucial to understand the structure of the radially excited heavy meson states. Experimental searches for these states in B, B^*, B_s, and B_s^* are thus highly anticipated.

The top panel of Fig. 3 shows the mass spectra of the 1S and 2S state heavy mesons. The middle panel of Fig. 3 represents the mass gaps between the 1S and 2S state mesons and the four different contributions to this mass gap

$(\Delta M^{\rm Kin}, \Delta M^{\rm Conf}, \Delta M^{\rm Coul}, \Delta M^{\rm Hyp})$ are depicted in the bottom panel of Fig. 3. The dashed and solid lines in the upper and middle panels represent our results obtained with the pure $(\theta = 0^\circ)$ and mixed $(\theta = 12^\circ)$ cases, respectively. The decomposition of ΔM shown in the bottom panel of Fig. 3 is for the mixed case. We also note in this taxonomical analysis that the contributions of the heavier and lighter quarks in the kinetic energy part are further separated and denoted as "Kin 1" and "Kin 2," respectively, when the quark contents are different. As one can see from the mass gap ΔM, the observed mass gap relation, $\Delta M_P > \Delta M_V$, cannot be realized without introducing the mixing angle. It is also interesting to see from the available data that the mass gaps between the 1S and 2S states are around 600 MeV, and the values are almost flavor-independent. Similar mass gap is also observed for the radially excited states of baryons with various flavors [38].

While the mass gap ΔM seems almost flavor-independent as shown in the middle panel of Fig. 3, the four different contributions, $(\Delta M_{\rm Kin}, \Delta M_{\rm Conf}, \Delta M_{\rm Coul}, \Delta M_{\rm Hyp})$, which make up ΔM, are flavor-dependent as one can see from the bottom panel of Fig. 3. For instance, comparing the Coulomb and confinement interactions, one can easily find from Eq. (17) that $\Delta M_{\rm Conf} \propto \beta^{-1}$ while $\Delta M_{\rm Coul} \propto \beta$. This relation provides an intuitive explanation for the observation that the confinement is dominant at large distances, while the Coulomb interaction arising from

the one-gluon exchange dominates at short distances. This tendency can be clearly seen in the bottom panel of Fig. 3. By comparing the mass gap components of (η_c, η_b) or $(J/\psi, \Upsilon)$, one can see that the green area for ΔM_{Coul} becomes larger for bottom quark systems. We also find that the kinetic energy is one of the important components in the mass gap. In particular, for mesons with different quark and antiquark masses such as B and D mesons, we find that the light quark (Kin2) gains more kinetic energy than the heavy quark (Kin1) as one may expect intuitively.

III. APPLICATIONS

With the model parameters fixed by mass spectrum, we predict various properties of the $1S$ and $2S$ state heavy mesons in this section. The standard LFQM adopting the spin-orbit wave functions and the polarization vectors of a vector meson defined in Eqs. (10) and (11) is based on the requirement of all constituents being on their respective mass shell (i.e., $M \rightarrow M_0$). This on-mass-shell condition of quark and antiquark is completely different from the manifestly covariant models, which allow the quark and antiquark to be off-mass-shell allowing $M \neq M_0$. For instance, the invariant mass M_0 included in the polarization vector $\epsilon(0)$ of Eq. (11) in the standard LFQM needs to be replaced by the physical mass M in the manifestly covariant model.

The complications coming from the binding energy issue do not appear in the analysis of meson mass spectra since only the radial wave functions are needed. However, it does matter for the calculations of other physical observables such as the decay constants and form factors, which we will discuss below. In the previous works of Refs. [39–43] for the decay constants, DAs for pseudoscalar and vector mesons, and weak transition form factors between two pseudoscalar mesons, it was shown that the self-consistent LFQM description of those physical observables can be achieved if and only if every physical mass M appeared in the matrix elements is replaced by the invariant mass M_0. In other words, the replacement of the physical mass M in the integrand of the amplitude by the invariant mass M_0 (denoted by CJ-scheme for convenience) results in the physical observables that are independent of the current components and polarizations used in the analysis. This $M \rightarrow M_0$ mapping is indeed proven to be an effective way of including the treacherous points such as the light-front zero modes and the instantaneous contributions. As the comprehensive and rigorous analysis of decay constants and DAs for pseudoscalar and vector mesons can be found in Refs. [39–42], here we just summarize the final theoretical results for those physical quantities for completeness.

A. Decay constants

The decay constants of a pseudoscalar meson P and a vector meson V with a four-momentum P^μ and a mass M are defined by

$$\langle 0|\bar{q}\gamma^\mu\gamma_5 q|P\rangle = if_P P^\mu,$$
$$\langle 0|\bar{q}\gamma^\mu q|V(P,\lambda)\rangle = f_V M\epsilon^\mu(\lambda), \quad (21)$$

as f_P and f_V, respectively, where $\epsilon^\mu(\lambda)$ is the polarization vector of a vector meson given by Eq. (11). For the case of pseudoscalar mesons, it has been explicitly shown that the decay constants of the pure $1S$ state mesons obtained from the plus $(\mu = +)$ and minus $(\mu = -)$ components of the currents are exactly the same [42]. In the present work, we extend it to the cases of mixed $1S$ and $2S$ states. Denoting $f_P^{(\pm)}$ obtained from the plus and minus components of the currents, the explicit forms of $f_P^{(\pm)}$ are given by [42]

$$f_P^{(\pm)} = \sqrt{6} \int_0^1 dx \int \frac{d^2\mathbf{k}_\perp}{(2\pi)^3} \frac{\Phi(x,\mathbf{k}_\perp)}{\sqrt{\mathcal{A}^2 + \mathbf{k}_\perp^2}} \mathcal{O}_P^{(\pm)}, \quad (22)$$

where $\mathcal{A} = (1-x)m_q + xm_{\bar{q}}$ and

$$\mathcal{O}_P^+ = \mathcal{A},$$
$$\mathcal{O}_P^- = \frac{\mathbf{k}_\perp^2 \mathcal{A}' + m_q m_{\bar{q}} \mathcal{A}}{x(1-x)M_0^2}, \quad (23)$$

with $\mathcal{A}' = \mathcal{A}(m_q \leftrightarrow m_{\bar{q}})$. Here, $\Phi(x,\mathbf{k}_\perp)$ denotes the wave functions (Φ_{1S}, Φ_{2S}) defined in Eq. (13) for $(1S, 2S)$ state decay constants.

For the vector meson case, it was also explicitly shown that the decay constants for the pure $1S$ state mesons obtained from the plus $(\mu = +)$ component of the currents with the longitudinal polarization $\epsilon(0)$ and the perpendicular $(\mu = \perp)$ components of the currents with the transverse polarizations $\epsilon(\pm)$ are exactly the same to each other [39]. Denoting f_V obtained from the plus and perpendicular components of the currents as $f_V^{(+)}$ and $f_V^{(\perp)}$, respectively, their explicit forms read [39]

$$f_V^{(+,\perp)} = \sqrt{6} \int_0^1 dx \int \frac{d^2\mathbf{k}_\perp}{(2\pi)^3} \frac{\Phi(x,\mathbf{k}_\perp)}{\sqrt{\mathcal{A}^2 + \mathbf{k}_\perp^2}} \mathcal{O}_V^{(+,\perp)}, \quad (24)$$

where

$$\mathcal{O}_V^+ = \mathcal{A} + \frac{2\mathbf{k}_\perp^2}{D_{\mathrm{LF}}},$$
$$\mathcal{O}_V^\perp = \frac{1}{M_0}\left[\frac{\mathbf{k}_\perp^2 + \mathcal{A}^2}{2x(1-x)} - \mathbf{k}_\perp^2 + \frac{(m_q + m_{\bar{q}})}{D_{\mathrm{LF}}}\mathbf{k}_\perp^2\right], \quad (25)$$

and $D_{\mathrm{LF}} = M_0 + m_q + m_{\bar{q}}$. In Ref. [44], both $f_V^{(+)}$ and $f_V^{(\perp)}$ were computed in the BLFQ approach, but the two results are found to depend on the adopted component of the current, which was ascribed to the measure of rotational symmetry violation of the model. In our LFQM calculation, by using the CJ-scheme, however, we could confirm

numerically that $f_P \equiv f_P^{(+)} = f_P^{(-)}$ and $f_V \equiv f_V^{(+)} = f_V^{(\perp)}$ for both $(1S, 2S)$ state mesons.

B. Twist-2 distribution amplitudes

The twist-2 quark DAs, $\phi_{P(V)}^{\mathrm{tw}-2}(x)$, for pseudoscalar and vector mesons are related with the decay constants obtained from the plus component of the currents through [45]

$$\int_0^1 \phi_{P(V)}^{\mathrm{tw}-2}(x, \mu) dx = \frac{f_{P(V)}^{(+)}}{2\sqrt{6}}, \tag{26}$$

where $\phi_{P(V)}^{\mathrm{tw}-2}(x, \mu)$ is obtained by the $\mathbf{k}_\perp$ integration of the LF wave function up to the transverse momentum scale μ. Here, $\mu(\geq |\mathbf{k}_\perp|)$ can be regarded as the energy scale that separates the perturbative and nonperturbative regimes. The twist-2 DA then describes the probability amplitudes to find the hadron in a state with a minimum number of Fock constituents and small transverse momentum separation. While the typical transverse momentum cutoff for the light meson sectors [39–41] was estimated as $\mu \approx 1$ GeV, the values of the scale μ for the heavy meson sectors appear shifted to the larger values as we discuss in the numerical results of Sec. IV B.

The normalized quark DA is defined as $\tilde{\phi}_{P(V)}^{\mathrm{tw}-2}(x, \mu) = (2\sqrt{6}/f_{P(V)}^{(+)})\phi_{P(V)}^{\mathrm{tw}-2}(x, \mu)$ so that

$$\int_0^1 \tilde{\phi}_{P(V)}^{\mathrm{tw}-2}(x, \mu) dx = 1. \tag{27}$$

The quark DAs can be usually expanded in Gegenbaur polynomials $C_n^{3/2}$ as $\tilde{\phi}(x, \mu) = \tilde{\phi}_{\mathrm{as}}(x)[1 + \sum_{n=1}^\infty a_n(\mu)C_n^{3/2}(\xi)]$, where the Gegenbaur moments $a_n(\mu)$ gauge the deviation of the DAs from the asymptotic one $\tilde{\phi}_{\mathrm{as}}(x) = 6x(1-x)$. Alternatively, one can define the expectation value of the longitudinal momentum, i.e., the $\xi = x - (1-x) = 2x - 1$ moments defined as [45]

$$\langle \xi^n \rangle = \int_0^1 dx \xi^n \tilde{\phi}_{P(V)}^{\mathrm{tw}-2}(x, \mu), \tag{28}$$

which are closely related with the Gegenbaur moments $a_n(\mu)$. The explicit relations between $\langle \xi^n \rangle$ and $a_n(\mu)$ can be found, for example, in Ref. [45].

C. Electromagnetic form factors and charge radii

We also compute the electromagnetic form factors of heavy pseudoscalar mesons as well as their charge radii. Our calculation is carried out by using the Drell-Yan-West frame $(q^+ = 0)$ with $\mathbf{q}_\perp^2 = Q^2 = -q^2$. The electromagnetic form factor of the pseudoscalar meson can be expressed for the "+" component of the current J^μ as [10]

$$F(Q^2) = e_q I^+(Q^2, m_q, m_{\bar{q}}) + e_{\bar{q}} I^+(Q^2, m_{\bar{q}}, m_q), \tag{29}$$

where $e_q(e_{\bar{q}})$ is the electric charge of quark (antiquark), and

$$I^+(Q^2, m_q, m_{\bar{q}}) = \int_0^1 dx \int \frac{d^2\mathbf{k}_\perp}{2(2\pi)^3} \Phi(x, \mathbf{k}_\perp)\Phi^*(x, \mathbf{k}'_\perp)$$
$$\times \frac{\mathcal{A}^2 + \mathbf{k}_\perp \cdot \mathbf{k}'_\perp}{\sqrt{\mathcal{A}^2 + \mathbf{k}_\perp^2}\sqrt{\mathcal{A}^2 + \mathbf{k}'^2_\perp}}, \tag{30}$$

where $\mathbf{k}'_\perp = \mathbf{k}_\perp + (1-x)\mathbf{q}_\perp$. The electromagnetic form factor is normalized as $F(0) = e_q + e_{\bar{q}}$, and the charge radius of the meson is given by

$$\langle r^2 \rangle = -6 \frac{dF(Q^2)}{dQ^2}\bigg|_{Q^2=0}. \tag{31}$$

IV. RESULTS AND DISCUSSION

A. Decay constants

In Fig. 4, we present our numerical results for the decay constants of the $1S$ (middle panel) and $2S$ (upper panel) state heavy mesons. The results obtained with the pure $(\theta = 0°)$ and mixed $(\theta = 12°)$ wave functions are represented by triangles and squares, respectively. For comparison, we show the available experimental data [23] and other theoretical predictions from lattice simulations [46–50] and the QCD sum rules [51].

While the decay constants of the $1S$ state mesons are rather robust against the change of the mixing angle, those of the $2S$ state mesons are shown to be quite sensitive to the mixing angle, and clearly a better description is achieved by taking into account the mixing effects. For instance, our predictions for the heavy quarkonia obtained with the mixed wave functions are $(f_{J/\Psi(1S)}, f_{J/\Psi(2S)}) = (390, 274)$ MeV and $(f_{\Upsilon(1S)}, f_{\Upsilon(2S)}) = (666, 498)$ MeV. These values not only satisfy the hierarchy of $f_{1S} > f_{2S}$ but also consistent with the experimental data [23]: $(f_{J/\Psi(1S)}^{\mathrm{Expt.}}, f_{J/\Psi(2S)}^{\mathrm{Expt.}}) = (407(5), 294(5))$ MeV and $(f_{\Upsilon(1S)}^{\mathrm{Expt.}}, f_{\Upsilon(2S)}^{\mathrm{Expt.}}) = (689(5), 497(5))$ MeV. The full numerical results of our LFQM compared with the available experimental data [23] as well as other theoretical model predictions [12,14,15,33,52–58] are summarized in Tables III and IV.

Displayed in the third panel of Fig. 4 are our results on the ratio $R_f = f_{2S}/f_{1S}$ obtained with $\theta = 0°$, $6°$, and $(12 \pm 1)°$ cases, which are compared with the available experimental data [23] and the lattice simulations [49]. In particular, we present the results with $\theta = (12 \pm 1)°$ as a band to check the sensitivity of the ratio R_f on the variation of the mixing angle around $\theta = 12°$. As one can see from the experimental data for $(J/\psi, \Upsilon)$, R_f should be less than unity for heavy meson systems. The same constraint, $R_f < 1$, for light mesons was also discussed in Ref. [9]. In our case with the pure state $(\theta = 0°)$, most heavy mesons except (D, D_s, η_c) mesons violate the constraint $R_f < 1$. For the critical mixing
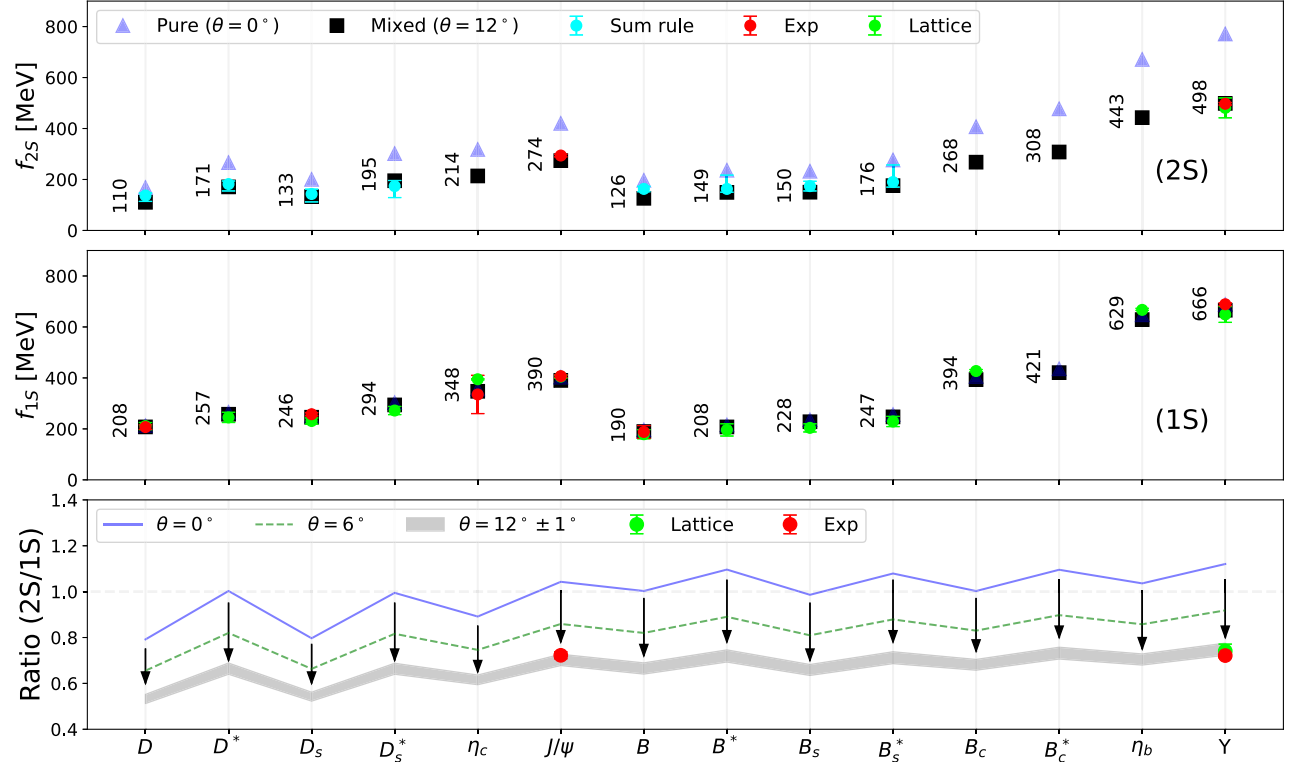
FIG. 4.   Upper and middle panels: comparison of the predicted decay constants of the 1S and 2S state heavy mesons with experimental data [23] and lattice simulations [46–49]. For the 2S state, we include the QCD sum rule result of Ref. [51]. Lower panel: the ratio $R_f = f_{2S}/f_{1S}$ compared to the experimental data and lattice simulations.

($\theta = \theta_c = 6°$) case, one can see that the constraint $R_f < 1$ is satisfied for all heavy mesons. However, the predictions with this critical mixing angle are still not comparable with the available experimental data. For our optimum mixing angle $\theta = 12°$, our results R_f for ($J/\psi, \Upsilon$), i.e.,

$R_{J/\psi[\Upsilon]} = 0.70[0.75]$ are now quite close to the data, $R_{J/\psi[\Upsilon]}^{\text{Expt.}} = 0.72[0.72]$ [23]. As for the sensitivity check of the mixing angle, we applied the larger mixing angle such as $\theta = 17.6°$ but obtained $R_{J/\psi[\Upsilon]} = 0.57[0.61]$, which underestimates the experimental data [23].

TABLE III.   Decay constants of the 1S and 2S heavy-light mesons in the units of MeV.

	$f_{D(1S)}$	$f_{D^*(1S)}$	$f_{D_s(1S)}$	$f_{D_s^*(1S)}$	$f_{B(1S)}$	$f_{B^*(1S)}$	$f_{B_s(1S)}$	$f_{B_s^*(1S)}$
Pure ($\theta = 0°$)	212	265	251	303	196	215	235	256
Mixed ($\theta = 12°$)	208	257	246	294	190	208	228	247
Expt. [23]	206.7 ± 8.9	…	257.5 ± 6.1	…	188 ± 25	…	…	…
Lattice [50]	211 ± 14	245 ± 20	231 ± 12	272 ± 16	179 ± 18	196 ± 24	204 ± 16	229 ± 20
Sum rules [52]	208 ± 10	263 ± 21	240 ± 10	308 ± 21	194 ± 15	213 ± 18	231 ± 16	255 ± 19
BS [53]	230 ± 25	340 ± 23	248 ± 27	375 ± 24	196 ± 29	238 ± 18	216 ± 32	272 ± 20
BS [54]	223(11)	…	242(8)	…	201(18)	…	253(17)	…
LFQM (CJ) [12]	197	239	233	274	171	186	205	220
LFQM (CJ2) [14]	208	230	232	260	181	185	205	216
LFQM [15]	197	230	219	253	163	172	184	194
RQM [55]	234	310	268	315	189	219	218	251
	$f_{D(2S)}$	$f_{D^*(2S)}$	$f_{D_s(2S)}$	$f_{D_s^*(2S)}$	$f_{B(2S)}$	$f_{B^*(2S)}$	$f_{B_s(2S)}$	$f_{B_s^*(2S)}$
Pure ($\theta = 0°$)	168	266	200	301	197	236	232	276
Mixed ($\theta = 12°$)	110	171	133	195	126	149	150	176
Sum rules, set I [51]	137^{+10}_{-23}	182^{+12}_{-27}	143^{+19}_{-31}	174^{+22}_{-45}	163^{+10}_{-11}	163^{+54}_{-13}	174^{+19}_{-19}	190^{+67}_{-20}
Sum rules, set II [51]	138^{+10}_{-22}	183^{+13}_{-24}	146^{+12}_{-36}	178^{+30}_{-39}	166^{+9}_{-10}	165^{+46}_{-12}	178^{+19}_{-17}	194^{+57}_{-18}
RQM [59]	292.14	293.38	…	…	…	…	…	…

TABLE IV.   Decay constants of the 1S and 2S state B_c and heavy quarkonia in the units of MeV.

	$f_{\eta_c(1S)}$	$f_{J/\Psi(1S)}$	$f_{B_c(1S)}$	$f_{B_c^*(1S)}$	$f_{\eta_b(1S)}$	$f_{\Upsilon(1S)}$
Pure ($\theta = 0°$)	356	403	406	436	647	688
Mixed ($\theta = 12°$)	347	390	393	421	629	666
Expt. [23]	335 ± 75	407 ± 5	...	...	...	689 ± 5
Lattice [46–49]	394.7 ± 2.4	405 ± 6	427^{+6}_{-2}	...	667^{+6}_{-2}	649 ± 31
RQM [56]	...	...	410 ± 20	...	...	...
Sum rules [57]	387 ± 7	418 ± 9	...	...	...	...
BS [53]	292 ± 25	459 ± 28	...	...	...	496 ± 20
BS [54]	385	...	519(1)	...	709	...
LFQM (CJ) [12]	326	360	349	369	507	529
LFQM (CJ2) [14]	353	361	389	391	605	611

	$f_{\eta_c(2S)}$	$f_{\Psi'(2S)}$	$f_{B_c(2S)}$	$f_{B_c^*(2S)}$	$f_{\eta_b(2S)}$	$f_{\Upsilon(2S)}$
Pure ($\theta = 0°$)	318	420	407	477	671	771
Mixed ($\theta = 12°$)	214	274	268	308	443	498
Expt. [23]	...	294(5)	...	...	...	497(5)
Lattice [49]	...	...	...	...	...	481(39)
BLFQ [58]	299(68)	312(73)	...	...	524(58)	518(48)
LFD [33]	...	288(6)	...	...	...	...

Further experimental measurements on the 2S decay constants are, therefore, highly desirable for testing our mixing angle effects.

B. Twist-2 distribution amplitudes

Shown in Fig. 5 are the normalized twist-2 DAs, $\tilde{\phi}_{P(V)}^{\text{tw}-2}(x, \mu)$, for the 1S and 2S state heavy pseudoscalar and vector mesons with $\theta = 12°$. Since the qualitative behaviors obtained with the pure ($\theta = 0°$) states are not much different from the mixed case, we do not give the results for the pure case in Fig. 5. In this figure, the convention is chosen so that the heavier quark in $(Q\bar{q})$ configuration carries the longitudinal momentum fraction x

and the lighter quark carries the fraction of $1 - x$. The DAs for the 1S state heavy pseudoscalar and vector mesons are given by the black solid and red dashed lines, respectively. We also compare our results for 1S pseudoscalar heavy mesons with the results of Ref. [60] (brown dot-dashed lines) obtained by employing a continuum approach to the hadron bound-state problem.

The DAs for 1S state heavy pseudoscalar mesons are not much different from those for the corresponding vector mesons within our LFQM mainly because the β parameters are same for both pseudoscalar and vector mesons. Although some quantitative differences can be found, in particular, for the B_c and heavy-light mesons, the
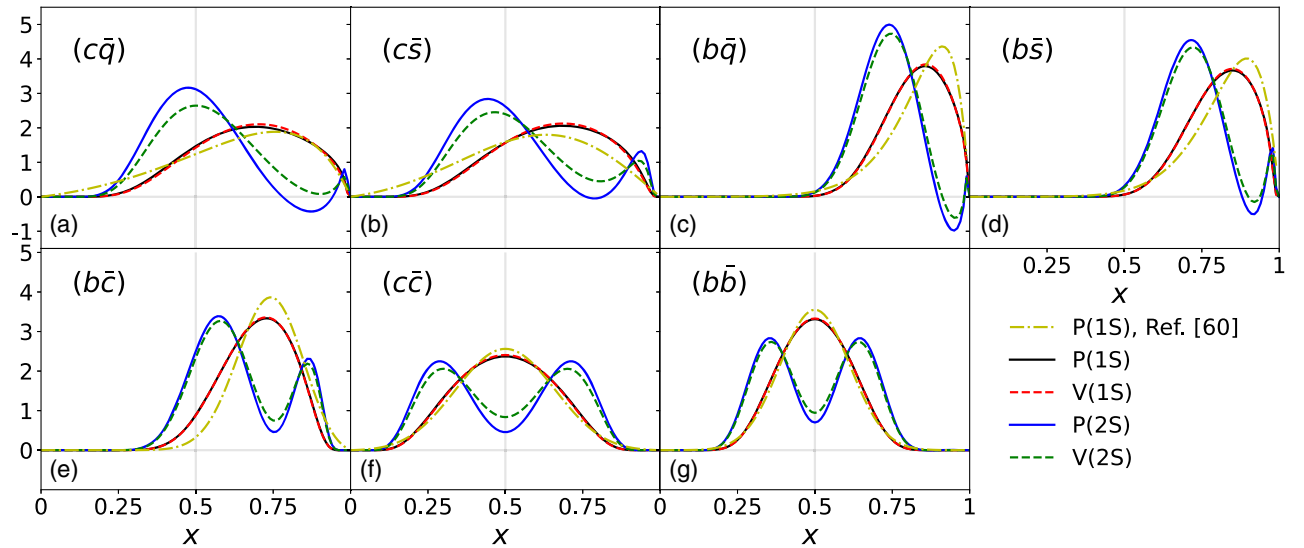

FIG. 5.   Distribution amplitude of the pseudoscalar (P) and vector (V) mesons of 1S and 2S states with the mixing angle $\theta = 12°$. The distribution amplitudes of the 1S pseudoscalar heavy meson predicted in Ref. [60] are shown for comparison.

qualitative behaviors of our results for pseudoscalar mesons are similar to those of Ref. [60]. For the 1S state heavy quarkonia ($c\bar{c}$, $b\bar{b}$), although both DAs are symmetric under $x \rightarrow 1 - x$, the shape of the DA is narrower for the bottomonium than the charmonium. However, the DAs for heavy-light systems become more asymmetric and more sharply peaked as the mass difference between the two constituents grows. In particular, one can see that the peak of the DA for heavy-heavy system such as the B_c is more attracted to the center compared to the heavy-light system.

The DAs of the 2S state pseudoscalar and vector mesons are shown by the blue solid and green dashed lines, respectively, in Fig. 5. This shows that the differences between pseudoscalar and vector mesons are more pronounced for the 2S states than for the 1S states. This tendency is opposite to that of BLFQ results [61] where the differences are more pronounced for the 1S states. We also found that the locations of the two extrema for the quarkonia systems move toward the endpoints as the quark mass decreases. In addition, the valley of the DAs is found to be much lower than those in Ref. [61]. Finally, we mention that the DAs for 2S state light meson sector such as (π, K) reported in Ref. [62] show similar qualitative behaviors found in the present work for the 2S state heavy mesons.

The normalized twist-2 pseudoscalar and vector meson DAs are rewritten as

$$\tilde{\phi}_{P(V)}^{\text{tw}-2}(x, \mu) = \int_0^{|\mathbf{k}_\perp| < \mu} d^2 \mathbf{k}_\perp \Psi_{P(V)}^{\text{tw}-2}(x, \mathbf{k}_\perp), \quad (32)$$

where the LF wave function corresponding to $\tilde{\phi}_{P(V)}^{\text{tw}-2}(x, \mu)$ is denoted as $\Psi_{P(V)}^{\text{tw}-2}(x, \mathbf{k}_\perp)$. Shown in Fig. 6 are the 3-dimensional (3D) plots of $\Psi_{P(V)}^{\text{tw}-2}(x, \mathbf{k}_\perp)$ and $\Psi_{\eta_c}^{\text{tw}-2}(x, \mathbf{k}_\perp)$ for the 2S states of D and η_c mesons, respectively. Equation (32) implies that the normalized twist-2 DAs $\tilde{\phi}_{P(V)}^{\text{tw}-2}(x, \mu)$ shown in Fig. 5 are obtained by the $\mathbf{k}_\perp$-integration of $\Psi_{P(V)}^{\text{tw}-2}(x, \mathbf{k}_\perp)$. In our LFQM calculation with the Gaussian wave functions, we observe that $|\mathbf{k}_\perp| \rightarrow \infty$ corresponds to the ultraviolet (UV) cutoffs ($k_\perp^{\text{max}}$) or energy scale μ around 2 GeV for ($D_{(s)}$, $B_{(s)}$, η_c), 3 GeV for B_c, and 4 GeV for η_b, respectively. In other words, the wave functions for heavy-heavy systems have longer transverse momentum tails than for the heavy-light systems. On the other hand, the wave functions for heavy-light systems have deeper negative valleys than for heavy-heavy systems. This property in the twist-2 light-front wave function explains why only the twist-2 DAs for the 2S state heavy-light system have negative regions. Of course, the small UV cutoff such as $|k_\perp^{\text{max}}| < 2$ GeV for heavy-heavy system may cause $\tilde{\phi}_P^{\text{tw}-2}(x)$ to have negative regions as well. Similar observations are made for the 2S state vector meson DAs.
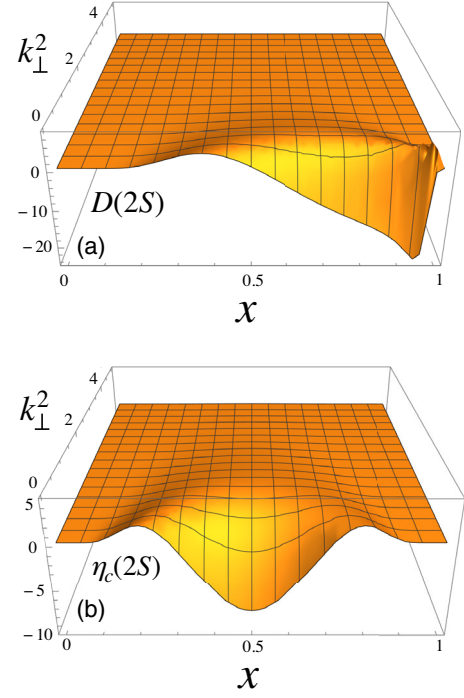

FIG. 6. 3D plots of (a) $\Psi_D^{\text{tw}-2}(x, \mathbf{k}_\perp)$ for the 2S states of the D meson and (b) $\Psi_{\eta_c}^{\text{tw}-2}(x, \mathbf{k}_\perp)$ for the 2S states of the η_c meson.

In Table V, we provide the ξ-moments defined in Eq. (28) up to $n = 6$ for both 1S and 2S state heavy mesons. For heavy quarkonia, the odd-n moments vanish because of the symmetric shape in their DAs. For heavy-light mesons, the odd-n moments reflect the asymmetry of the DAs coming from the mass difference between the quark and antiquark. As one can see, the first ξ moment decreases as $(m_Q - m_{\bar{q}})$ gets smaller. For example, we have $\langle \xi^1 \rangle_{B_q(1S)} = 0.644$, $\langle \xi^1 \rangle_{B_s(1S)} = 0.614$, and $\langle \xi^1 \rangle_{B_c(1S)} = 0.390$. The DAs for 1S state mesons can be well reproduced with the first few ξ moments up to $n = 4$. However, those for 2S state mesons require much higher ξ moments beyond $n = 6$ to reproduce the full results. For the 2S state D mesons, the first and third moments $\langle \xi^n \rangle_{D(2S)}$ ($n = 1, 3$) have negative values. This originates from the fact that the DA of $D(2S)$ occupies more in the $0 < x < 0.5$ domain compared to the other DAs. In addition, our predictions of $(\langle \xi^2 \rangle, \langle \xi^4 \rangle, \langle \xi^6 \rangle) = (0.179, 0.048, 0.019)$ for the 2S state of η_c are comparable to (0.16, 0.046, 0.016) of Ref. [63], which are obtained from the leading twist light-front wave functions with the Cornell potential.

C. Electromagnetic form factors and radii

In Fig. 7, we present the electromagnetic form factors of 1S (solid lines) and 2S (dashed lines) state heavy pseudoscalar mesons obtained with $\theta = 12°$. For comparison, we show the available lattice simulation data of Refs. [64–66]. Since the form factors of heavy quarkonia (η_c, η_b) obtained

TABLE V.   The ξ-moment up to $n = 6$ for the 1S and 2S state heavy pseudoscalar and vector mesons.

(1S)	D	D^*	D_s	D_s^*	η_c	J/ψ	B	B^*	B_s	B_s^*	B_c	B_c^*	η_b	Υ
$\langle\xi^1\rangle$	0.337	0.344	0.294	0.296	...	...	0.644	0.646	0.614	0.614	0.390	0.390	...	...
$\langle\xi^2\rangle$	0.226	0.226	0.197	0.194	0.088	0.086	0.453	0.454	0.417	0.417	0.201	0.201	0.049	0.049
$\langle\xi^3\rangle$	0.145	0.144	0.114	0.112	...	...	0.337	0.338	0.302	0.301	0.113	0.112	...	...
$\langle\xi^4\rangle$	0.108	0.107	0.083	0.080	0.018	0.017	0.261	0.262	0.228	0.227	0.068	0.068	0.006	0.006
$\langle\xi^5\rangle$	0.082	0.080	0.058	0.056	...	...	0.209	0.210	0.178	0.177	0.043	0.043	...	...
$\langle\xi^6\rangle$	0.065	0.063	0.044	0.042	0.005	0.005	0.172	0.172	0.143	0.142	0.029	0.028	0.001	0.001
(2S)	D	D^*	D_s	D_s^*	η_c	J/ψ	B	B^*	B_s	B_s^*	B_c	B_c^*	η_b	Υ
$\langle\xi^1\rangle$	−0.042	0.071	0.015	0.085	...	...	0.426	0.452	0.411	0.433	0.275	0.285	...	...
$\langle\xi^2\rangle$	0.052	0.096	0.132	0.140	0.179	0.160	0.198	0.227	0.202	0.224	0.160	0.162	0.099	0.094
$\langle\xi^3\rangle$	−0.004	0.034	0.055	0.064	...	...	0.094	0.121	0.112	0.130	0.101	0.100	...	...
$\langle\xi^4\rangle$	0.012	0.033	0.065	0.064	0.048	0.042	0.043	0.067	0.070	0.084	0.071	0.069	0.016	0.015
$\langle\xi^5\rangle$	0.006	0.022	0.047	0.045	...	...	0.017	0.037	0.048	0.059	0.051	0.049	...	...
$\langle\xi^6\rangle$	0.010	0.020	0.044	0.040	0.016	0.014	0.004	0.021	0.036	0.045	0.038	0.036	0.003	0.003

from both quark and antiquark contributions vanish, we show only the contribution from the quark part for the comparison with the available lattice simulation results. This shows that our results for the 1S state (D^+, D_s^+, η_c) mesons match well with the lattice simulation results. We find that the form factors of 2S state mesons are in general steeper than those for the corresponding 1S state mesons. In a heavy-light system such as $(D_{(s)}^+, B^+)$, the main contribution to the form factor for the region of $Q^2 > 6$ GeV^2

comes from the heavy quark and the light quark contribution is negligible at high Q^2 regions. On the other hand, for the form factor of the B_c meson, both b and c quark contributions are almost equally important for the intermediate Q^2 region.

Figure 8 presents the calculated charge radii $\langle r_{nS}^2 \rangle$ of the $(1S, 2S)$ state heavy mesons obtained with $\theta = 0°$ and $\theta = 12°$ cases by triangles and boxes, respectively. Since there are no experimental data, our results are compared
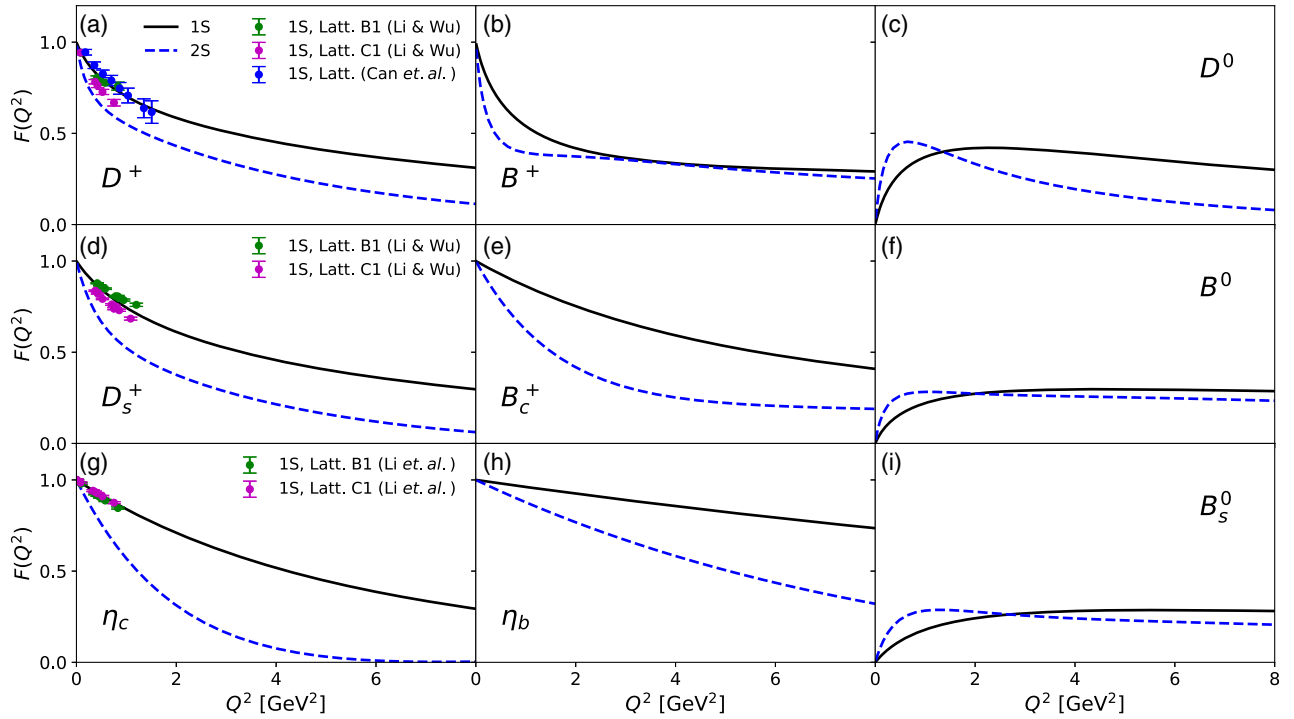

FIG. 7.   Electromagnetic form factor of the 1S and 2S state heavy pseudoscalar mesons. The available lattice simulations are also shown by blue circles for the results of Ref. [64], and green circles and magenta circles for B1 and C1 ensembles of Refs. [65,66], respectively. Only one quark contribution is considered for quarkonia.
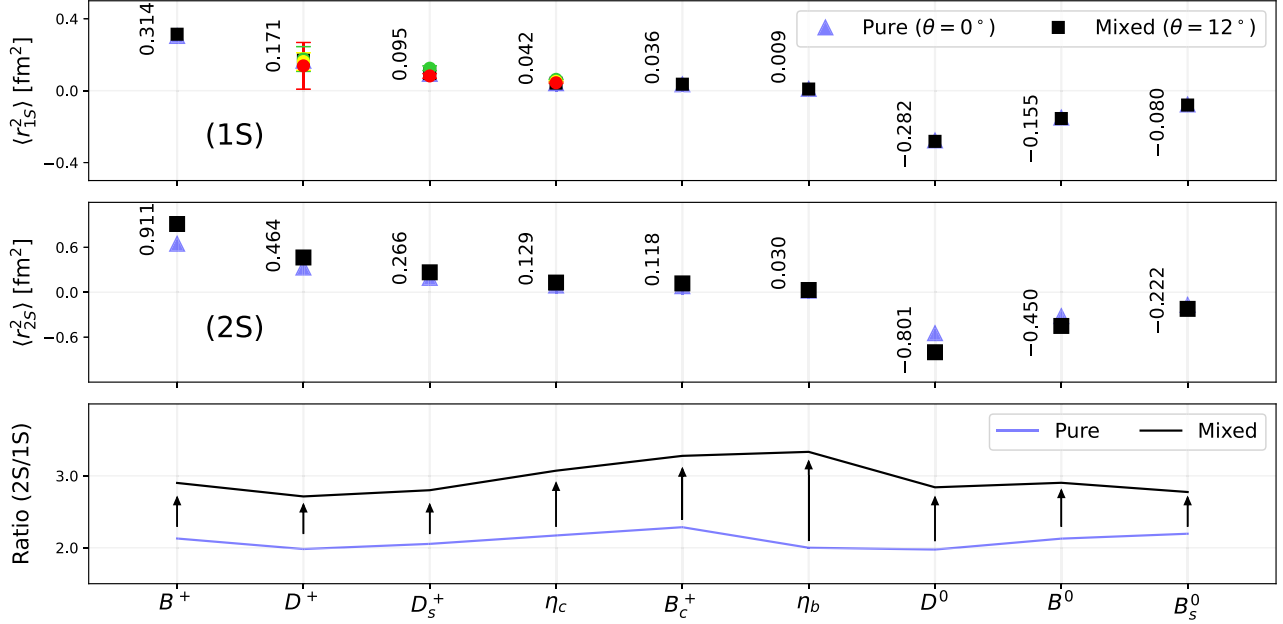
FIG. 8. Upper and middle panels: charge radii of the 1S and 2S state heavy mesons with various quark flavor contents. Our predictions for 1S heavy mesons have a good agreement with the lattice simulation data of Refs. [64–67]. Lower panel: the ratio of the charge radii $R_r = \langle r_{2S}^2 \rangle / \langle r_{1S}^2 \rangle$ for various heavy mesons. The charge radii in the mixed state are larger than the pure ones.

with the lattice simulation results of Refs. [64–67]. The results of Fig. 8 are summarized in Table VI with other model predictions from Refs. [6,58,68]. We find that our predictions are overall in a good agreement with the lattice results. Since the heavy quark is sitting near the center of a meson while the light quark is moving actively, the radius of a heavy-light meson would be mostly governed by the motion of the light quark. This can be noticed by comparison with the results of the LFQM of Ref. [6].

We find that the charge radii for 2S state mesons are more sensitive to the mixing angle than for the 1S state

cases. As shown in Fig. 8, the charge radii for 2S state mesons are larger in the mixed case than those in the pure one. The larger radii can be understood from the 2S wave functions given in Fig. 2. Namely, the reduction of the wave function at the origin results in a larger radius since the wave function is more spreading to a larger distance. This is the opposite behavior of the decay constants shown in Fig. 4, which is proportional to the wave function at the origin. Therefore, these observables reflect the structure of the wave functions from different points of view.

TABLE VI. Charge radii of the 1S and 2S pseudoscalar heavy mesons in the units of fm^2.

$\langle r^2 \rangle$	$B^+(1S)$	$D^+(1S)$	$D_s^+(1S)$	$\eta_c(1S)$	$B_c^+(1S)$	$\eta_b(1S)$	$D^0(1S)$	$B^0(1S)$	$B_s^0(1S)$
Pure ($\theta = 0°$)	0.304	0.166	0.093	0.041	0.035	0.010	−0.277	−0.150	−0.077
Mixed ($\theta = 12°$)	0.314	0.171	0.095	0.042	0.036	0.009	−0.282	−0.155	−0.080
Lattice, Linear fit [64]	...	0.138(13)	...	...	...	...	...	...	...
Lattice, Quadratic fit [64]	...	0.152(26)	...	...	...	...	...	...	...
Lattice, B1 [65,66]	...	0.162(49)	0.082(13)	0.052(4)	...	...	...	...	...
Lattice, C1 [65,66]	...	0.176(69)	0.125(13)	0.044(4)	...	...	...	...	...
Lattice, [67]	...	...	...	0.063(1)	...	...	...	...	...
CCQM [68]	...	0.255	0.142	...	...	...	...	...	...
LFQM [6]	0.378	0.184	0.124	...	0.0433	...	−0.304	−0.187	−0.119
	0.496	0.248	0.181	...	...	...	−0.496	−0.248	−0.181
BLFQ [58]	...	...	...	0.027	...	0.012	...	...	...
$\langle r^2 \rangle$	$B^+(2S)$	$D^+(2S)$	$D_s^+(2S)$	$\eta_c(2S)$	$B_c^+(2S)$	$\eta_b(2S)$	$D^0(2S)$	$B^0(2S)$	$B_s^0(2S)$
Pure ($\theta = 0°$)	0.647	0.329	0.191	0.089	0.080	0.020	−0.547	−0.319	−0.169
Mixed ($\theta = 12°$)	0.911	0.464	0.266	0.129	0.118	0.030	−0.801	−0.450	−0.222
BLFQ [58]	...	...	...	0.120	...	0.050	...	...	...

V. SUMMARY

In the present work, we have investigated $1S$ and $2S$ state heavy mesons employing the pure and mixed harmonic oscillator wave functions. We invoked the variational principle adopting the linear plus Coulomb potential, and treated the hyperfine interaction perturbatively as a contact term to distinguish vector and pseudoscalar mesons. The variational principle allowed us to obtain a constraint for model parameters. With the fixed quark masses, all model parameters are determined by two meson masses and this led us to predict and test other physical quantities.

We have analyzed the mass spectra, decay constants, distribution amplitudes, electromagnetic form factors, and charge radii of the $1S$ and $2S$ state heavy mesons. As for the mass spectra, our predictions are in a good agreement with the available experimental data. Although no apparent difference is found for the masses of the $1S$ heavy mesons in the pure and mixed cases, the predicted masses of the $2S$ heavy mesons are appreciably modified and have a better agreement with the available data when the mixing is introduced. Our results support the speculation that the newly observed $D_{s0}(2590)^+$ by the LHCb Collaboration [16] can be interpreted as the radially excited $D_s(2S)$ state.

We also observe that the mass gaps between the $1S$ and $2S$ state mesons are around 600 MeV and they are not sensitive to the flavor contents of mesons. In LFQM, we found that mass gaps of pseudoscalar mesons can be made larger than those of vector mesons regardless of the quark flavor contents only if we use the mixing angle $\theta \geq \theta_c = 6°$. Such behavior can be explained by Eq. (19), which shows that the hierarchy appears in the opposite direction without mixing.

The mixing effects are crucial to understand the properties of $2S$ state mesons. As for the decay constants, we could obtain a good agreement with the experimental and lattice simulation data for $1S$ state mesons even without the mixing effects. However, for the $2S$ states, the mixing effects are essential to get the correct order of decay constants. By introducing a small mixing, we noticed that the ratio $R_\Phi = \Phi_{2S}^2/\Phi_{1S}^2$ becomes smaller than unity. The optimum value of the mixing angle is obtained as $12°$ to cover both the charm and bottom flavors of the heavy quark. In principle, one may include ϕ_{3S} with two more mixing parameters to maintain the orthogonality of $1S$, $2S$ and $3S$ meson states. According to our analysis in this work, however, since the mixing effect impacts the $1S$ state far less than the $2S$ state as one can clearly see from Eq. (13) with our optimum value of $\theta = 12°$, it was sufficient to impose just one mixing angle for the analysis up to the $2S$ meson states.

For the DAs of the $1S$ states, our prediction is found to be similar to those reported in Ref. [54]. For the $2S$ states, some DAs have the nodal structure arising from the structure of the wave functions. We note that the difference between DAs for vector and pseudoscalar mesons are more pronounced for the $2S$ states. In addition, we find that the DAs are saturated up to several GeV for the transverse momentum and it has longer tails for mesons with heavier quarks. For completeness, the corresponding ξ-moments up to $n = 6$ are computed in the present work.

The electromagnetic form factors and charge radii for D, D_s, and η_c mesons are also computed and found to be comparable with the available lattice simulation data of Refs. [64–66]. The mixing effects lead to larger radii of the $2S$ states since their wave functions are more spread in space, which results in the reduction of the wave functions near the origin. This is opposite to the behavior of the decay constants that are reduced by the mixing.

In this work, we have focused on the heavy meson sector in LFQM. However, a combined analysis for both light and heavy meson sectors is also of great importance for scrutinizing the dependence of physical quantities on quark masses. In the future work, we would consider smearing the hyperfine interaction to treat it nonperturbatively as a part of the entire Hamiltonian for the application of the variational principle. A global analysis would be also required for more rigorous investigations to discuss the uncertainties of the model parameters. While the investigation along this directions is under progress, more precise measurements on the physical properties of heavy mesons as well as observations of undiscovered heavy meson states are essential to test phenomenological models on the structure of heavy mesons.

[1] P. A. M. Dirac, Forms of relativistic dynamics, Rev. Mod. Phys. **21,** 392 (1949).

[2] S. J. Brodsky, H.-C. Pauli, and S. S. Pinsky, Quantum chromodynamics and other field theories on the light cone, Phys. Rep. **301,** 299 (1998).

[3] W. Jaus, Semileptonic decays of B and D mesons in the light-front formalism, Phys. Rev. D **41,** 3394 (1990).

[4] W. Jaus, Covariant analysis of the light-front quark model, Phys. Rev. D **60,** 054026 (1999).

[5] H.-Y. Cheng, C.-Y. Cheung, C.-W. Hwang, and W.-M. Zhang, Covariant light-front model of heavy mesons within heavy quark effective theory, Phys. Rev. D **57,** 5598 (1998).

[6] C.-W. Hwang, Charge radii of light and heavy mesons, Eur. Phys. J. C **23,** 585 (2002).

[7] H.-W. Ke, X.-Q. Li, Z.-T. Wei, and X. Liu, Restudy on the wave functions of $\Upsilon(nS)$ states in the light-front quark model and the radiative decays of $\Upsilon(nS) \rightarrow \eta_b + \gamma$, Phys. Rev. D **82,** 034023 (2010).

[8] Q. Chang, X.-N. Li, X.-Q. Li, F. Su, and Y.-D. Yang, Self-consistency and covariance of light-front quark models: Testing via P, V, and A meson decay constants, and $P \rightarrow P$ weak transition form factors, Phys. Rev. D **98,** 114018 (2018).

[9] D. Arndt and C.-R. Ji, Light-cone quark model analysis of radially excited pseudoscalar and vector mesons, Phys. Rev. D **60,** 094020 (1999).

[10] H.-M. Choi and C.-R. Ji, Mixing angles and electromagnetic properties of ground state pseudoscalar and vector meson nonets in the light-cone quark model, Phys. Rev. D **59,** 074015 (1999).

[11] H.-M. Choi and C.-R. Ji, Light-front quark model analysis of exclusive $0^- \rightarrow 0^-$ semileptonic heavy meson decays, Phys. Lett. B **460,** 461 (1999).

[12] H.-M. Choi and C.-R. Ji, Semileptonic and radiative decays of the B_c meson in the light-front quark model, Phys. Rev. D **80,** 054016 (2009).

[13] H.-M. Choi, Decay constants and radiative decays of heavy mesons in light-front quark model, Phys. Rev. D **75,** 073016 (2007).

[14] H.-M. Choi, C.-R. Ji, Z. Li, and H.-Y. Ryu, Variational analysis of mass spectra and decay constants for ground state pseudoscalar and vector mesons in the light-front quark model, Phys. Rev. C **92,** 055203 (2015).

[15] N. Dhiman, H. Dahiya, C.-R. Ji, and H.-M. Choi, Twist-2 pseudoscalar and vector meson distribution amplitudes in light-front quark model with exponential-type confining potential, Phys. Rev. D **100,** 014026 (2019).

[16] R. Aaij et al. (LHCb Collaboration), Observation of a New Excited D_s^+ Meson in $B^0 \rightarrow D^- D^+ K^+ \pi^-$ Decays, Phys. Rev. Lett. **126,** 122002 (2021).

[17] S. Godfrey and N. Isgur, Mesons in a relativized quark model with chromodynamics, Phys. Rev. D **32,** 189 (1985).

[18] D. Ebert, R. N. Faustov, and V. O. Galkin, Properties of heavy quarkonia and B_c mesons in the relativistic quark model, Phys. Rev. D **67,** 014027 (2003).

[19] D. Ebert, R. N. Faustov, and V. O. Galkin, Heavy-light meson spectroscopy and Regge trajectories in the relativistic quark model, Eur. Phys. J. C **66,** 197 (2010).

[20] Z. Gao, G. Y. Wang, Q. F. Lü, J. Zhu, and G. F. Zhao, Canonical interpretation of the $D_{s0}(2590)^+$ resonance, Phys. Rev. D **105,** 074037 (2022).

[21] P. G. Ortega, J. Segovia, D. R. Entem, and F. Fernández, The $D_{s0}(2590)^+$ as the dressed $c\bar{s}(2^1S_0)$ meson in a coupled-channels calculation, Phys. Lett. B **827,** 136998 (2022).

[22] J.-M. Xie, M.-Z. Liu, and L.-S. Geng, $D_{s0}(2590)$ as a dominant $c\bar{s}$ state with a small D^*K component, Phys. Rev. D **104,** 094051 (2021).

[23] P. A. Zyla et al. (Particle Data Group), The review of particle physics, Prog. Theor. Exp. Phys. **2020,** 083C01 (2020).

[24] L. D. Roper, Evidence for a P_{11} Pion-Nucleon Resonance at 556 MeV, Phys. Rev. Lett. **12,** 340 (1964).

[25] A. J. Arifi, D. Suenaga, A. Hosaka, and Y. Oh, Strong decays of multistrangeness baryon resonances in the quark model, Phys. Rev. D **105,** 094006 (2022).

[26] E. Klempt and A. Zeitsev, Glueball, hybrids, multiquarks: Experimental facts versus QCD inspired concepts, Phys. Rep. **454,** 1 (2007).

[27] M. B. Voloshin and M. A. Shifman, On the annihilation constants of mesons consisting of a heavy and a light quark, and $B^0 \leftrightarrow \bar{B}^{-0}$ oscillations, Sov. J. Nucl. Phys. **45,** 292 (1987).

[28] M. B. Voloshin and M. A. Shifman, On production of D^* and D mesons in B-meson decays, Sov. J. Nucl. Phys. **47,** 511 (1988).

[29] N. Isgur and M. B. Wise, Weak decays of heavy mesons in the static quark approximation, Phys. Lett. B **232,** 113 (1989).

[30] N. Isgur and M. B. Wise, Weak transition form-factors between heavy mesons, Phys. Lett. B **237,** 527 (1990).

[31] C.-W. Hwang, Study of quark distribution amplitudes of 1S and 2S heavy quarkonium states, Eur. Phys. J. C **62,** 499 (2009).

[32] T. Peng and B.-Q. Ma, Heavy quarkonium 2S states in the light-front quark model, Eur. Phys. J. A **48,** 66 (2012).

[33] M. Li, Y. Li, G. Chen, T. Lappi, and J. P. Vary, Light-front wavefunctions of mesons by design, arXiv:2111.07087.

[34] N. Isgur, D. Scora, B. Grinstein, and M. B. Wise, Semileptonic B and D decays in the quark model, Phys. Rev. D **39,** 799 (1989).

[35] D. Scora and N. Isgur, Semileptonic meson decays in the quark model: An update, Phys. Rev. D **52,** 2783 (1995).

[36] R. Aaij et al. (LHCb Collaboration), Precise measurements of the properties of the $B_1(5721)^{0,+}$ and $B_2^*(5747)^{0,+}$ states and observation of $B^{+,0}\pi^{-,+}$ mass structures, J. High Energy Phys. 04 (2015) 024.

[37] T. Aaltonen et al. (CDF Collaboration), Study of orbitally excited B mesons and evidence for a new $B\pi$ resonance, Phys. Rev. D **90,** 012013 (2014).

[38] A. J. Arifi, H. Nagahiro, A. Hosaka, and K. Tanida, Roper-like resonances with various flavor contents and their two-pion emission decays, Phys. Rev. D **101,** 111502(R) (2020).

[39] H.-M. Choi and C.-R. Ji, Self-consistent covariant description of vector meson decay constants and chirality-even quark-antiquark distribution amplitudes up to twist 3 in the light-front quark model, Phys. Rev. D **89,** 033011 (2014).

[40] H.-M. Choi and C.-R. Ji, Consistency of the light-front quark model with chiral symmetry in the pseudoscalar meson analysis, Phys. Rev. D **91,** 014018 (2015).

[41] H.-M. Choi and C.-R. Ji, Two-particle twist-3 distribution amplitudes of the pion and kaon in the light-front quark model, Phys. Rev. D **95,** 056002 (2017).

[42] H.-M. Choi, Self-consistent light-front quark model analysis of $B \to D\ell\nu_\ell$ transition form factors, Phys. Rev. D **103,** 073004 (2021).

[43] H.-M. Choi, Current-component independent transition form factors for semileptonic and rare $D \to \pi(K)$ decays in the light-front quark model, Adv. High Energy Phys. **2021,** 4277321 (2021).

[44] M. Li, Y. Li, P. Maris, and J. P. Vary, Radiative transitions between 0^{-+} and 1^{--} heavy quarkonia on the light front, Phys. Rev. D **98,** 034024 (2018).

[45] H.-M. Choi and C.-R. Ji, Distribution amplitudes and decay constants for (π, K, ρ, K^*) mesons in the light-front quark model, Phys. Rev. D **75,** 034019 (2007).

[46] C. McNeile, C. T. H. Davies, E. Follana, K. Hornbostel, and G. P. Lepage, Heavy meson masses and decay constants from relativistic heavy quarks in full lattice QCD, Phys. Rev. D **86,** 074503 (2012).

[47] C. T. H. Davies, C. McNeile, E. Follana, G. P. Lepage, H. Na, and J. Shigemitsu (HPQCD Collaboration), Update: Precision D_s decay constant from full lattice QCD using very fine lattices, Phys. Rev. D **82,** 114504 (2010).

[48] G. C. Donald, C. T. H. Davies, R. J. Dowdall, E. Follana, K. Hornbostel, J. Koponen, G. P. Lepage, and C. McNeile (HPQCD Collaboration), Precision tests of the J/ψ from full lattice QCD: Mass, leptonic width, and radiative decay rate to η_c, Phys. Rev. D **86,** 094501 (2012).

[49] B. Colquhoun, R. Dowdall, C. Davies, K. Hornbostel, and G. Lepage (HPQCD Collaboration), Υ and Υ' leptonic widths, a_μ^b, and m_b from full lattice QCD, Phys. Rev. D **91,** 074514 (2015).

[50] D. Becirevic, Ph. Boucaud, J. P. Leroy, V. Lubicz, G. Martinelli, F. Mescia, and F. Rapuano, Nonperturbatively improved heavy-light mesons: Masses and decay constants, Phys. Rev. D **60,** 074501 (1999).

[51] P. Gelhausen, A. Khodjamirian, A. A. Pivovarov, and D. Rosenthal, Radial excitations of heavy-light mesons from QCD sum rules, Eur. Phys. J. C **74,** 2979 (2014).

[52] Z.-G. Wang, Analysis of the masses and decay constants of the heavy-light mesons with QCD sum rules, Eur. Phys. J. C **75,** 427 (2015).

[53] G. Cvetič, C. S. Kim, G.-L. Wang, and W. Namgung, Decay constants of heavy meson of 0^- state in relativistic Salpeter method, Phys. Lett. B **596,** 84 (2004).

[54] D. Binosi, L. Chang, M. Ding, F. Gao, J. Papavassiliou, and C. D. Roberts, Distribution amplitudes of heavy-light mesons, Phys. Lett. B **790,** 257 (2019).

[55] D. Ebert, R. N. Faustov, and V. O. Galkin, Relativistic treatment of the decay constants of light and heavy mesons, Phys. Lett. B **635,** 93 (2006).

[56] S. Capstick and S. Godfrey, Pseudoscalar decay constants in the relativized quark model and measuring the CKM matrix elements, Phys. Rev. D **41,** 2856 (1990).

[57] D. Bečirević, G. Duplančić, B. Klajn, B. Melić, and F. Sanfilippo, Lattice QCD and QCD sum rule determination of the decay constants of η_c, J/ψ and h_c states, Nucl. Phys. **B883,** 306 (2014).

[58] Y. Li, P. Maris, and J. P. Vary, Quarkonium as a relativistic bound state on the light front, Phys. Rev. D **96,** 016022 (2017).

[59] M. Shah, B. Patel, and P. C. Vinodkumar, D meson spectroscopy and their decay properties using Martin potential in a relativistic Dirac formalism, Eur. Phys. J. C **76,** 36 (2016).

[60] F. E. Serna, R. C. da Silveira, J. J. Cobos-Martínez, B. El-Bennich, and E. Rojas, Distribution amplitudes of heavy mesons and quarkonia on the light front, Eur. Phys. J. C **80,** 955 (2020).

[61] S. Tang, Y. Li, P. Maris, and J. P. Vary, Heavy-light mesons on the light front, Eur. Phys. J. C **80,** 522 (2020).

[62] B.-L. Li, L. Chang, F. Gao, C. D. Roberts, S. M. Schmidt, and H.-S. Zong, Distribution amplitudes of radially-excited π and K mesons, Phys. Rev. D **93,** 114033 (2016).

[63] V. V. Braguta, Study of leading twist light cone wave functions of $2S$ state charmonium mesons, Phys. Rev. D **77,** 034026 (2008).

[64] K. U. Can, G. Erkol, M. Oka, A. Ozpineci, and T. T. Takahashi, Vector and axial-vector couplings of D and D^* mesons in $2 + 1$ flavor lattice QCD, Phys. Lett. B **719,** 103 (2013).

[65] N. Li and Y.-J. Wu, Lattice study of D and D_s meson form factors with twisted boundary conditions, Eur. Phys. J. A **53,** 56 (2017).

[66] N. Li, C.-C. Liu, and Y.-J. Wu, Lattice study of form factors for charmonium, Eur. Phys. J. A **56,** 242 (2020).

[67] J. J. Dudek, R. G. Edwards, and D. G. Richards, Radiative transitions in charmonium from lattice QCD, Phys. Rev. D **73,** 074507 (2006).

[68] R. M. Moita, J. P. B. C. de Melo, K. Tsushima, and T. Frederico, Exploring the flavor content of light and heavy-light pseudoscalars, Phys. Rev. D **104,** 096020 (2021).